Atherosclerotic conditions promote the packaging of functional microRNA-92 into endothelial microvesicles

Inaugural-Dissertation

zur Erlangung des Doktorgrades

der Hohen Medizinischen Fakultät

der Rheinischen Friedrich-Wilhelms-Universität

Bonn

Yangyang Liu

aus Bonn

2019

Angefertigt mit der Genehmigung
der Medizinischen Fakultät der Universität Bonn

1. Gutachter: Prof. Dr. Nikos Werner
2. Gutachter: Prof. Dr. Eike Latz

Tag der Mündlichen Prüfung: 29.01.2019

Aus der Medizinischen II - Innere Medizin (Kardiologie, Pneumologie)
Direktor: Prof. Dr. med. Georg Nickenig

Contents

List of abbreviations

CAD	coronary artery disease
MV	microvesicle
nm	nanometers
miR	microRNA
ECs	endothelial cells
EMV	endothelial cell-derived microvesicle
ACS	acute coronary syndrome
PMV	platelet-derived microvesicle
LMV	eukocyte-derived microvesicle
Ago2	argonaute-2
oxLDL	oxidized low-density lipoprotein
HCAEC	human coronary artery endothelial cell
BrdU	bromodeoxyuridine
DAPI	4′,6-diamidino-2-phenylindole
NCAD	no coronary artery disease
STAT3	signal transducer and activator of transcription 3
MMV	monocyte-derived microvesicle
Cy3	cyanine 3
THBS1	thrombospondin 1
RPLP0	ribosomal protein lateral stalk subunit P0
TEK	TEK receptor tyrosine kinase
ANGPT1	angiopoietin 1
ITGA5	integrin α5
PTEN	phosphatase and tensin homolog

1. Introduction

1.1 Coronary artery disease

Coronary artery disease (CAD) and its cardiovascular sequelae still represent the leading cause of mortality worldwide. The underlying disease, atherosclerosis, is characterized by a continuous damage of the vascular endothelium leading to endothelial activation and apoptosis, the development of endothelial dysfunction and subsequent atherosclerotic lesion formation. The initial step in the development of atherosclerosis is the damage of healthy endothelium and the exposure of vascular cells to various pathogenic factors. Decreasing of antithrombotic and anticoagulatory properties of normal endothelium contribute to the formation of atherosclerotic plaque. Additionally, endothelial dysfunction is associated with a couple of inflammatory factors which increase plaque vulnerability. Therefore, the dysfunctional endothelium plays key role in plaque destabilization and erosion in the development and progression of CAD(Lerman and Zeiher, 2005).

1.2 Circulating MV in CAD

As a consequence of endothelial activation and dysfunction, CAD patients show increased plasma level of circulating microvesicle (MV)(Boulanger, et al., 2012), which represent small membrane vesicles with a size of 100 to 1000 nanometers (nm). MV, also referred to as microparticle, can be released from most cell types (circulating cells, vascular cells, and cardiomyoctyes)(Camussi, et al., 2010). Both cell activation and cell apoptosis can lead to MV liberation from cells. MV retain surface molecules from parent cells, as well as part of their cytosolic content during their formation and shedding(Boulanger, et al., 2006). However, MV are not merely inert debris that reflects cellular activation or injury. In contrast, they are important carriers of bioactive molecules (proteins, mRNAs and microRNAs (miRs)) playing essential roles in cell–cell cross talk. By transferring their biological content into recipient cells, MV are regarded as crucial regulators of cardiovascular health and disease, including activation of platelets and

endothelial cells (ECs), as well as regulation of inflammation and coagulation(Ray, et al., 2008, Brill, et al., 2005, Owens and Mackman, 2011, Jansen, et al., 2013). Moreover, in human plasma, circulating MV have ideal characteristics as risk makers because they are stable and easily detectable by reliable quantitative techniques (annexin V capture assay and flow cytometry)(György, et al., 2011).

There is increasing evidence indicating that MV are emerging as key players in cardiovascular disease development and progression. In patients with stable CAD, coronary calcification or ACS, both of platelet-derived microvesicle (PMV) and EMV (endothelial cell-derived microvesicle) are elevated(Jayachandran, et al., 2008, Mallat, et al., 2000, Simak, et al., 2006). In asymoptomatic patients with subclinical atherosclerosis, in contrast, levels of MV originating from leukocytes are increased(Chironi, et al., 2006). Similar findings were observed in patients with heart failure and valvular disease. In these pathologies, EMV, PMV and LMV (leukocyte-derived microvesicle) levels also are increased. Notably, plasma MV levels are also associated with clinical outcomes in several cardiometabolic diseases, including coronary artery disease, chronic renal failure, diabetes mellitus, and obesity(Heiss, et al., 2008, Amabile, et al., 2005, Werner, et al., 2006, Koga, et al., 2005, Esposito, et al., 2006). Moreover, MV levels are modulated in other vascular diseases, including preeclampsia(González-Quintero, et al., 2003), inflammatory vasculitis(Brogan, et al., 2004), and antiphospholipid syndrome(Dignat-George, et al., 2004).

Atherosclerotic plaques contain large numbers of MV, mostly from lymphocyte and monocyte-macrophage cells, and their levels increase in patients with high atherothrombosis risk(Rautou, et al., 2011). Therefore, significant increases in plasma LMV levels are associated with unstable plaques. In addition, numerous studies have revealed that PMV may contribute to platelet activation during atherothrombosis(Del Conde, et al., 2005, Siljander, 2011, Shantsila, et al., 2010). A recent study found that PMV enhanced normal platelet activation, and PMV may be effective targets for preventing platelet activation in CAD(Wang, et al., 2012). Furthermore, abundant evidences demonstrated that plasma EMV level is a novel biomarker of endothelial dysfunction. Indeed, Schiro et al. showed that carotid artery disease is associated with significantly elevated plasma levels of EMV(Schiro, et al., 2014). Similarly,

Bernal-Mizrachi et al. reported that high levels of EMV were associated with high risk lesions with multiple thrombi in cardiovascular disease (Bernal-Mizrachi, et al., 2004). All together, these findings indicate that plasma levels of MV could be of prognostic value for the occurrence of cardiovascular diseases.

1.3 Circulating miRs in CAD

The first miR was discovered by Lee and colleagues in 1993, isolating Lin-4 from the nematode Caenorhabditis elegans(Lee, et al., 1993). Since then, more than 1,700 miRs have been identified (www.mirbase.org). miRs are a class of short, non-coding RNAs of 22 nucleotides length, and miRs negatively regulate gene expression posttranscriptionally through inhibiting translation from and/or inducing degradation of messenger RNAs(Lee and Ambros, 2001). Consequently, miRs have been associated with cardiovascular disease risk factors, such as myocardial infarction, atherosclerosis, CAD, heart failure, atrial fibrillation, hypertrophy and fibrosis(Fichtlscherer, et al., 2010, Small, et al., 2010, Corsten, et al., 2010, Gomes da Silva and Silbiger, 2014). Particularly, since miRs are significant regulators in inflammation, angiogenesis and apoptosis which are important characteristics of plaque vulnerability, they may play as key factors in atherosclerotic plaque formation and plaque rupture. Extracellularly circulating miRs are either associated with different types of vesicles (exosomes, MV, apoptotic bodies) or bound to proteins (high-density lipoprotein, argonaute-2 (Ago2)) apparently without being encapsulated into vesicles(Arroyo, et al., 2011, Turchinovich, et al., 2011). Notably, vesicle-associated miRs appeared to be more stable than those not associated with vesicles(Köberle, et al., 2013). In particular, previous studies indicated that cells can selectively package miRs into MV and secreted miRs can act as signaling molecules mediating cell-cell communication altering function and phenotype of the target cells(Jansen, et al., 2013, Zhang, et al., 2010). In addition, increasing evidence shows that circulating miRs are altered in diverse cardiovascular pathologies (Jansen, et al., 2016). Therefore, circulating miRs have emerged as a novel class of biomarkers for CAD patients(Loyer, et al., 2014). Importantly, high expressions of vasculoprotective miRs within MV show atheroprotective effects in experimental murine models of vascular injury and atherosclerosis(Jansen, et al., 2013, Zernecke, et al., 2009, Hergenreider, et al.,

2012) and are associated with a reduced rate of major adverse cardiovascular events in patients with stable CAD(Jansen, et al., 2014).

Whereas numerous studies explored the role of MV-bound miRs in patients with stable CAD, the influence of different stages of CAD (angiographically excluded CAD, stable CAD and ACS) on MV-miR expression is unclear.

As miR-containing MV regulate vascular function and disease progression, a detailed exploration of miRs expression in circulating MV in patients with stable CAD, acute coronary syndrome (ACS) and angiographically excluded CAD would be of high interest to better understand the pathogenesis of CAD and develop novel therapeutic strategies.

1.4 Aims

In this study, we aimed to explore the expression and role of circulating MV-miRs in patients with angiographically excluded CAD, stable CAD and ACS.

2. Material and Methods

2.1 Study subjects

Between August 2012 and July 2013, 233 patients presenting in our outpatient and emergency department were enrolled in the study. Informed consent was obtained from all patients and the ethics committee of the University of Bonn approved the study protocol (approval number 05/12). According to the results of clinical presentation, laboratory parameters and coronary angiography, patients were classified into 3 groups: angiographic exclusion of obstructive coronary artery disease (<50% stenosis of a major coronary artery, named as no CAD (NCAD), n=41), stable CAD (n=77) and acute coronary syndrome (ACS, n=62, Figure 1).

2.2 Preparation of blood samples

Venous blood was drawn under sterile conditions from the cubital vein and was buffered using sodium citrate (for MV quantification) or ethylenediaminetetraacetic acid (EDTA, for miR analysis). Additional blood samples for routine analyses were obtained. Blood was centrifuged at 1500*g* for 15 minutes followed by centrifugation at 13,000*g* for 2 minutes to generate platelet-deficient plasma. The deprived plasma samples were immediately stored in −80 °C. Annexin V/CD 31 positive MV levels were measured freshly with flow cytometry by using Annexin V-FITC and CD31-PE (BD Pharmingen). Platelet-deficient plasma was stored in −80 °C until miR levels were analyzed.

2.3 MV collection and RNA isolation

RNA was isolated from circulating MV by using TRIzol-based miR isolation protocol. 250 µl total plasma was centrifuged at 20,000*g* for 30 minutes at 4 °C to pellet circulating MV as previously described(Jansen, et al., 2013, Jansen, et al., 2014), (Jansen, et al., 2017). The pellet was diluted in 250 µl RNase-free water and then diluted in 750 µl TRIzol® LS in order to measure MV-miRs levels. *Caenorhabditis elegans* miR-39 (cel-miR-39, 5nM, Qiagen) was spiked in TRIzol for normalization of miR content as

described(Fichtlscherer, et al., 2010). To increase the yield of small RNAs, the RNA was precipitated in ethanol at −20 °C overnight with glycogen (Invitrogen).

2.4 Sorting of MV subspecies

For sorting of MV subspecies, 250 µl platelet-free plasma was stained with CD31-PE, and CD42b-APC (BD Pharmingen) and the corresponding isotype and negative controls. Stained plasma was incubated for 45 minutes in dark at room temperature according to the manufactures suggestions. To sort MV subspecies, a FACSAria™ III Flow Cytometer (BD Biosciences) was used. Vesicles between 100–1000 nm in diameter were gated for sorting. CD31+/CD42b−, CD31+/CD42b+ and CD31−/CD42b− MV were gated, sorted and collected as previously described(Jansen, et al., 2016, Jansen, et al., 2014). RNase-free water was added to the sorted MV to reach a total volume of 250 µl, which was diluted in 750 µl TRIzol® LS in order to measure MV-miRs levels. Cel-miR-39 was spiked in TRIzol for normalization of miR content as described(Jansen, et al., 2014). To increase the yield of small RNAs, the RNA was precipitated in ethanol at −20 °C overnight with glycogen (Invitrogen).

2.5 Quantification of miRs by quantitative PCR

RNA was quantified using Nanodrop spectrophotometer (Nanodrop Technologies Inc). 10 ng of the total RNA was reversely transcribed using TaqMan® miR reverse transcription kit (Applied Biosystems) according to the manufactures protocol. miR-126, miR-222, miR-let7, miR-21, miR-30, miR-92, miR-139, miR-199 and miR-26 in circulating MV were detected by using TaqMan® miR assays (Applied Biosystems) on a 7500 HT Real-Time PCR machine (Applied Biosystems). For all miRs, a Ct value above 40 was defined as undetectable. Values were normalized to cel-miR-39 and are expressed as $2^{-[CT(miR)-CT(cel\text{-}miR-39)]}$ log10. For all PCR experiments, samples were run in triplicates.

2.6 Cell culture and endothelial MV generation

Human coronary artery endothelial cells (HCAEC, PromoCell) were cultured in endothelial cells (ECs) growth media with endothelial growth media Supplement Mix (Promocell) under standard cell culture conditions (37 °C, 5 % CO_2). Cells of passage 4–7 were used when 70–80 % confluent. EMV were generated from HCAEC as previously described(Jansen, et al., 2013). Briefly, confluent cells were starved by subjecting to basal media without growth media supplements for 24 hours to induce apoptosis. After starvation, supernatant of apoptotic HCAEC was collected and centrifuged at 1500*g* for 15 minutes to remove cell debris. The supernatant was centrifuged (20,000*g*, 40 minutes) to pellet EMV. The obtained EMV were washed in sterile phosphate buffered saline (PBS, pH 7.4) and pelleted again at 20,000*g* for 40 minutes. Pelleted EMV were resuspended in sterile PBS and used freshly. For all experiments, EMV were used at a concentration of 2000/µl, which has been shown an effective concentration to explore functional effects of EMV in previous experiments(Jansen, et al., 2013, Rautou, et al., 2011, Jansen, et al., 2012).

2.7 miRs sorting in oxLDL EMV by quantitative PCR

In order to generate EMV from ECs under oxidized low-density lipoprotein (oxLDL) conditions, confluent HCAEC were stimulated with 50µg/ml oxLDL for 24 hours and then subjected to basal media without growth media supplements for 24 hours to generate EMV. EMV derived from oxLDL-treated HCAEC were defined as oxLDL EMV. Pelleted oxLDL EMV were resuspended in sterile PBS and used freshly. Total RNA was isolated out of oxLDL EMV by TRIzol® (Invitrogen) extraction method according to instruction of the manufacturer. To increase the yield of small RNAs, the RNA is precipitated in ethanol at −20 °C overnight with glycogen (Invitrogen). RNA was quantified using Nanodrop spectrophotometer (Nanodrop Technologies Inc). 10 ng of the total RNA was reversely transcribed using TaqMan® miR reverse transcription kit (Applied Biosystems) according to the manufactures protocol. miR-126, miR-222, miR-let7, miR-21, miR-30, miR-92, miR-139, miR-199 and miR-26 in oxLDL EMV were detected by using TaqMan® miR assays (Applied Biosystems) on a 7500 HT Real-Time PCR machine (Applied Biosystems). The data are presented as the fold change in miR expression normalized to

RNU6B (fold change = $2^{-\Delta\Delta CT}$). For all miRs, a Ct value above 40 was defined as undetectable. For all PCR experiments, samples were run in triplicates.

2.8 miR-92 expression in oxLDL EMV and oxLDL-treated HCAEC

In order to generate oxLDL EMV from HCAEC under different oxLDL concentrations, confluent HCAEC were stimulated with PBS, 10µg/ml, 20µg/ml, 50µg/ml and 100µg/ml oxLDL for 24 hours and then subjected to basal media without growth media supplements for 24 hours to generate different oxLDL EMV. Pelleted oxLDL EMV were resuspended in sterile PBS and used freshly. Total RNA was isolated out of oxLDL EMV and oxLDL-treated HCAEC by TRIzol® (Invitrogen) extraction method according to instruction of the manufacturer. To increase the yield of small RNAs, the RNA is precipitated in ethanol at −20 °C overnight with glycogen (Invitrogen). RNA is quantified using Nanodrop spectrophotometer. Then, 10 ng of the total RNA was reversely transcribed using TaqMan® miR reverse transcription kit (Applied Biosystems) according to the manufacturers protocol. Taqman® miR assays (Applied Biosystems) were used to measure miR-92 levels on a 7500 HT Real-Time PCR machine (Applied Biosystems). The data are presented as fold change in miR expression normalized to RNU6B (fold change = $2^{-\Delta\Delta CT}$).

2.9 STAT3 inhibition in vitro

HCAEC were pre-incubated with PBS (as control), 2µM/L, 4µM/L and 6µM/L Stattic (Calbiochem), a non-peptitic specific STAT3 inhibitor, for 4 hours and then subjected to basal media without growth media supplements for 24 hours to generate different EMV. Total RNA was isolated out of EMV and Stattic-treated HCAEC by TRIzol® (Invitrogen) extraction method according to instruction of the manufacturer. To increase the yield of small RNAs, the RNA is precipitated in ethanol at −20 °C overnight with glycogen (Invitrogen). RNA is quantified using Nanodrop spectrophotometer. Then, 10 ng of the total RNA was reversely transcribed using TaqMan® miR reverse transcription kit (Applied Biosystems) according to the manufacturers protocol. Taqman® miR assays (Applied Biosystems) were used to measure miR-92 levels on a 7500 HT Real-Time PCR

machine (Applied Biosystems). The data are presented as fold change in miR expression normalized to RNU6B (fold change = $2^{-\Delta\Delta CT}$).

2.10 Boyden chamber assay

HCAEC ($1*10^5$) were seeded onto the upper compartment of Boyden chambers (BD falcon) with transwell polycarbonate inserts (8.0µm pore size) for 24 hours. EMV, $EMV^{miR\text{-}92\text{-}downregulated}$, $EMV^{mock\text{-}transfected}$ or vehicle was added into the lower well of the Boyden chamber, incubating for 6 hours to allow for cell migration. The insert was removed, and the upper side of the insert, was scraped off with a rubber cell lifter. The inserts were fixed with 4% paraformaldehyde and stained with DAPI. Cell migration was quantified by counting cells of 3 random microscopic fields (×100) in each well.

2.11 Scratch Assay

HCAEC were grown to confluence and scratched with a sterile pipette (10ul). After the scratch, growth factor-deprived medium was added to the cells and cells were stimulated with 2000 AnnV+ EMV/µl, 2000 AnnV+ $EMV^{miR\text{-}92\text{-}downregulated}$ /µl, 2000 AnnV+ $EMV^{mock\text{-}transfected}$ /µl, or vehicle. Then, cells were photographed on a marked position at 0, 3 or 4 and 6 hours. The remaining cell free area was measured and correlated (in percent) to the initial scratched area.

2.12 HCAEC proliferation assay by fluorescence microscopy

HCAEC in basal medium were deprived of growth media supplements and coincubated with EMV, $EMV^{miR\text{-}92\text{-}downregulated}$, $EMV^{mock\text{-}transfected}$ or vehicle for 24 hours. Next, the cells were pulsed with BrdU (10µM, BD) for 6 hours. Cells were fixed and denatured. BrdU incorporation was detected using rat anti-BrdU (Abcam) and secondary antibody anti-rat-cy3 (Jackson ImmunoResearch). Nuclei were stained with DAPI (Vector labaratories). Zeiss Axiovert 200M microscope and AxioVision software were used to take photographs.

2.13 HCAEC proliferation assay by flow cytometry

HCAEC in basal medium were deprived of growth media supplements for 24 hours, followed by stimulation with EMV, $EMV^{miR\text{-}92\text{-}downregulated}$, $EMV^{mock\text{-}transfected}$ or vehicle in growth media with supplements for 24 hours. Cell cycle analysis was performed using Bromodeoxyuridine (BrdU) Flow Kit (BD) according to the instructions of the manufacturer. In brief, cells were pulsed with BrdU (10 μM) for 3 hours. Cells were trypsinated, fixed and permeabilized. BrdU incorporation was detected using FITC-conjugated anti-BrdU antibody for 20 minutes at room temperature followed by incubation with 7-aminoactinomycin (7-AAD) viability staining solution in staining buffer overnight at 4 °C. Stained cells were analyzed using FACSCalibur (BD).

2.14 HCAEC tube formation assay

HCAEC tube formation was assessed with an assay based on the use of a growth factor reduced (GFR) Matrigel. After thawing overnight at 4°C, 250 μL GFR Matrigel was placed into each well of cold 24-well plates using cold pipette tips, and the GFR Matrigel was allowed to incubation for 30 minutes in room temperature. HCAEC were placed in the wells coated with GFR Matrigel at $4*10^4$ cells per well in deprived of growth media supplements and coincubated with EMV, $EMV^{miR\text{-}92\text{-}downregulated}$, $EMV^{mock\text{-}transfected}$ or vehicle for 24 hours under standard cell culture conditions (37 °C, 5 % CO2). Wells containing PBS were used as controls. Four randomly selected fields of view were analyzed, and tube formation was quantified by measuring the number of junctions and the number of nodes. Digital images of microtiter wells sections were obtained using Zeiss Axiovert 200M microscope. Data were analyzed with the Image-Pro Plus software.

2.15 Taqman miR array

RNA (more than 500ng) was converted to cDNA by priming with a mixture of looped primers (Human Mega Plex Primer Pools, Applied Biosystems). MiR profiles in isolated MV from stable CAD (n=5) and ACS (n=5) patients were assessed using TaqMan® Array miR Cards (Applied Biosystems) for a total of 384 unique assays specific to human miRs

under standard real-time PCR conditions. PCR was carried out on an Applied Biosystems 7900HT thermocycler using the manufacturer's recommended program. Detailed analysis of the results was performed using the Data Analysis v3.0 Software (Applied Biosystems). CT values above 35 were defined as undetectable.

2.16 RT2 Profiler PCR Array Gene Expression

HCAEC were pre-incubated with EMV, $EMV^{miR\text{-}92\text{-}downregulated}$, $EMV^{mock\text{-}transfected}$ or vehicle for 24 hours. Total RNA was isolated out of HCAEC by TRIzol (QIAGEN) extraction method according to instruction of the manufacturer. RNA is quantified using Nanodrop spectrophotometer. Then, more than 500ng of the total RNA was reversely transcribed using RT2 First Strand Kit (QIAGEN) according to the manufacturers protocol. RT² Profiler PCR array analysis was performed to measure the expression of 84 key genes involved in modulating the biological processes of angiogenesis. PCR was carried out on an Applied Biosystems 7500 HT real-time PCR machine. Detailed data analysis report was performed using the Data Analysis v3.0 Software (Applied Biosystems) and exported from the QIAGEN web portal at GeneGlobe. CT values above 35 were defined as undetectable.

2.17 Transfection of HCAEC

To generate $EMV^{miR\text{-}92\text{-}downregulated}$ and $EMV^{mock\text{-}transfected}$, HCAEC were transfected with miR-92 inhibitor (1nM, all from Applied Biosystems) using lipofectamine 2000 (Invitrogen) for 24 hours and exposed to media without growth media supplements for 24 hours to generate modified EMV. For siRNA experiments, HCAEC were transfected with THBS1 siRNA or control siRNA (5nM, Thermo Fisher Scientific) using lipofectamine 2000 for 24 hours. Functional assays were performed in 48 hours.

2.18 EMV-incorporated miR-92 were absorbed into recipient ECs

HCAEC ($1*10^5$) were transfected with 20 nM of cyanine 3 (Cy3)-labeled miR-92 (Riboxx) using HiPerFect (QIAGEN). The day after transfection, ECs were washed three times with PBS, and the medium was switched to serum-free medium. After incubation for 24 hours, the serum-free culture medium was collected and used for EMV generation as previously described(Jansen, et al., 2013, Rautou, et al., 2011, Jansen, et al., 2012). Then EMV were labeled with PKH67 (Sigma-Aldrich) according to the manufacturer's instructions. PKH67-labeled EMV were washed twice with PBS. To further evaluate the uptake of EMV into cultured ECs, ECs were incubated with PKH67-labeled EMV for 6 hours. And then nuclei were stained with 4′,6-diamidino-2-phenylindole（DAPI，Vector labaratories）. Zeiss Axiovert 200M microscope and AxioVision software were used to visualize the uptake of EMV-incorporated miR-92 into recipient ECs.

2.19 miR-92 expression calculation in target ECs using copy number

HCAEC in basal medium were deprived of growth media supplements and coincubated with EMV, $EMV^{miR\text{-}92\text{-}downregulated}$, $EMV^{mock\text{-}transfected}$ or vehicle for 24 hours. The absolute expression of miR-92 was determined by obtaining standard curves with different concentration of miR-92 mimic (Applied Biosystems) as templates. Logarithmic values of oligonucleotide concentrations and Ct values were plotted. The copy number was calculated from the oligonucleotide concentration and the molecular mass of the transcript as described(Jansen, et al., 2013).

2.20 Western Blot

HCAEC in basal medium were deprived of growth media supplements and coincubated with EMV, $EMV^{miR\text{-}92\text{-}downregulated}$, $EMV^{mock\text{-}transfected}$ or vehicle for 48 hours. Then, HCAEC were homogenized with RIPA buffer (150 mM NaCl, 1.0% Nonidet P-40, 0.5% deoxycholate, 0.1% SDS, and 50 mM Tris, pH 8.0) containing 1 mM Na3VO4, 5mM NaF and protease inhibitor cocktail (Roche) at 4°C. Protein concentration was measured using Lowry protein assay (BioRad). Equal amounts of proteins (30 μg) were loaded into 12% SDS electrophoresis, transferred onto PVDF membranes and blocked with 5% dry

milk for 1 hour. Blots were incubated with the appropriate primary antibodies: anti-thrombospondin 1 (anti-THBS1, Abcam); anti-GAPDH (Hytest). Detection was performed using the appropriate secondary antibody (Anti-Rabbit IgG H,L (HRP), Abcam) and proteins were revealed by chemiluminescence using the ECL kit (GE healthcare). GAPDH was used as the loading control.

2.21 Target mRNA expression analysis by real-time PCR

HCAEC in basal medium were deprived of growth media supplements and co-incubated with EMV, $EMV^{miR\text{-}92\text{-}downregulated}$, $EMV^{mock\text{-}transfected}$ or vehicle for 24 hours. Total RNA was isolated out of HCAEC by TRIzol (Invitrogen) extraction method according to instruction of the manufacturer. RNA was quantified using Nanodrop spectrophotometer. Then, 1µg of the isolated total RNA was reversely transcribed using Omniscript reverse transcription kit (QIAGEN) according to the manufacturer's protocol. The expression of the following 3 genes (Assay ID; Applied Biosystems) were quantified using a 7500 Fast Real-Time PCR System: THBS1 ((Hs00962908_m1); TEK (Hs00945146_m1); ANGPT1(Hs00919202_m1). The data was presented as the fold change in mRNA expression normalized to GAPDH (fold change = $2^{-\Delta\Delta CT}$).

2.22 Statistical analysis

Normally distributed continuous variables were presented as mean ± SD. Continuous variables were tested for normal distribution with the use of the Kolmogorov–Smirnov test. Categorical variables are given as frequencies and percentages. For continuous variables, Student t test or Mann-Whitney U was used for comparison between 2 groups. For the comparison of >2 groups, the 1-way ANOVA with Bonferroni’s correction for multiple comparisons test was used. The Chi square test was used for categorical data that result from classifying objects. Binary logistic regression was applied to identify factors that were independently associated with miR-92. All tests were 2-sided, and statistical significance was assumed when the null hypothesis could be rejected at

$p < 0.05$. Statistical analysis was performed with IBM SPSS Statistics version 20 (USA) and GraphPad Prism 7.

All authors attest to the accuracy and completeness of the data and all analyses and confirm that the study was conducted according to the protocol.

3. Results

3.1 Study design

Between August 2012 and July 2013, 233 patients presenting with symptoms of stable CAD or ACS in our outpatient and emergency department were enrolled in the study. To identify alterations of MV-miR expression between stable CAD and ACS patients, we first performed miR screening. Specifically, miR profile in isolated circulating MV from stable CAD (n=5) and ACS patients (n=5) was assessed using taqman miR array. To validate miR array results, another 223 patients were screened for inclusion. Among those, 43 patients with malignant (n=8), inflammatory diseases (n=15), severe hepatic or renal dysfunction (n=13) or declination of participation (n=7) were excluded from the study. Finally, a total of 180 patients were prospectively included (Figure 1). Patients were classified into 3 groups: Angiographic exclusion of obstructive coronary artery disease (<50% stenosis of a major coronary artery, named as no CAD (NCAD), n=41), stable CAD (n=77) and acute coronary syndrome (ACS, n=62, Figure 1, Table 1).

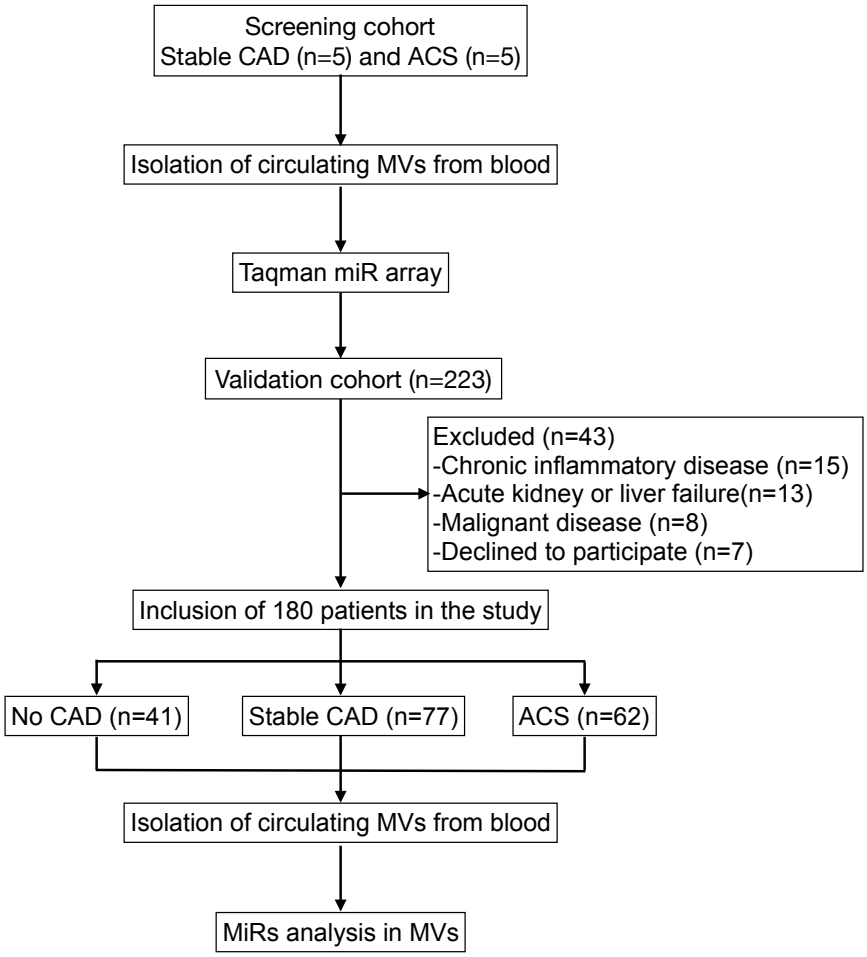

Fig. 1: Study flow

According to the study protocol, we first performed miR screening. MiR profile in isolated circulating MV from stable CAD (n=5) and ACS patients (n=5) were assessed using taqman miR array. To validate miR array results, a total of 180 patients with angiographically excluded CAD (n=41), stable CAD (n=77) and ACS (n=62) were prospectively included in the study. Circulating MV were isolated from patients' plasma using ultracentrifugation. MiRs derived from MV were analyzed by real-time PCR. CAD indicates coronary artery disease; ACS, acute coronary syndrome; MV, microvesicle; MiR, microRNA.

3.2 Baseline characteristics

There was no difference regarding age among the three groups. Most of the patients (68.9%) enrolled were male, which was driven by higher numbers of male patients in the stable CAD and ACS group (*P*=0.001)

Stable CAD and ACS patients were more likely to have diabetes (*P*=0.042), hyperlipoproteinemia (*P*=0.043), and a lower left ventricular ejection fraction (*P*=0.004) compared to NCAD patients. Stable CAD and ACS patients took more frequently ACE inhibitors, beta blockers, statins, aspirin and clopidogrel. Regarding the laboratory parameters, serum creatinine, glucose, HbA1c, glomerular filtration rate, triglycerides, LDL cholesterol and C-reactive protein leucocytes levels were similar in the three groups. Stable CAD and ACS patients showed reduced cholesterol (*P*=0.003) and HDL cholesterol (*P*=0.001) levels compared to NCAD patients (Table 1).

Tab. 1: Baseline characteristics of the study population

Characteristic	Total (n=180)	NCAD (n=41)	Stable CAD (n=77)	ACS (n=62)	P value
Age. year	65.3±11.3	63.4± 13.2	65.3±10.6	66.5±10.9	0.413
Gender. no. (%)					0.001
Female	56(31.1%)	26(63.4%)	12(15.6%)	18(29.0%)	
male	124(68.9%)	15(36.6%)	65(84.4%)	44(71.0%)	
Cardiovascular risk factors. (%)					
Arterial hypertension	141(78.3%)	30(73.2%)	60(77.9%)	51(82.3%)	0.545
Hyperlipoproteinemia	94(52.2%)	16(39.0%)	39(50.6%)	39(62.9%)	0.043
Family history	43(24.2%)	11(26.8%)	18(23.4%)	14(22.6%)	0.876
Diabetes	55(30.6%)	7(12.2%)	23(29.1%)	25(40.3%)	0.042
Smoking	43(23.9%)	7(17.1%)	24(31.2%)	14(22.6%)	0.209
Body mass index. kg/m2	27.9±11.3	26.6±6.0	28.2±3.9	28.3±5.6	0.183
Medical history. (%)					
Previous bypass	21(11.7%)	0(0%)	9(11.7%)	12(19.4%)	0.011
Previous MI (6 months)	45(25.0%)	0(0%)	33(42.9%)	12(19.4%)	0.001
Previous stroke	7(3.9%)	2(4.9%)	1(1.3%)	4(6.5%)	0.275
Chronic kidney disease	6(3.3%)	2 (4.9%)	1(1.3%)	3(4.8%)	0.421
PCI					
Previous	101(56.1%)	0 (0%)	61(79.2%)	40 (64.5%)	0.001
Current	90(50.0%)	0(0%)	48(62.3%)	42(67.7%)	0.001
Coronary artery disease. no. (%)					0.001
1 Vessels	28(15.6%)	0(0%)	16(20.8%)	12(19.4%)	
2 Vessels	48(26.7%)	0(0%)	29(37.7%)	19(30.6%)	
3 Vessels	63(35.0%)	0(0%)	32(41.6%)	31(50.0%)	
Left ventricular ejection fraction. %	57.4±12.3	62.8±8.9	55.8±10.8	55.2±15.0	0.004
Medication on admission. no. (%)					
ACE inhibitors	114(63.3%)	14(34.1%)	58(75.3%)	42(67.7%)	0.001
Angiotensin receptor blockers	34(18.9%)	10(24.4%)	11(14.3%)	13(21.0%)	0.359
Beta blockers	150(83.3%)	25(61.0%)	69(89.6%)	56(90.3%)	0.001
Calcium channel blockers	33(18.3%)	7(17.1%)	11(14.3%)	15(24.2%)	0.315
Diuretics	77(42.8%)	21(51.2%)	27(35.1%)	29(46.8%)	0.176
Statins	148(82.2%)	15(36.5%)	75(97.4%)	58(93.5%)	0.001
Nitrates	9(5.0%)	1(2.4%)	5(6.5%)	3(4.8%)	0.628
Aspirin	140(77.8%)	8(19.5%)	75(97.4%)	57(91.9%)	0.001
Clopidogrel	54(30.0%)	1(2.4%)	23(29.9%)	30 (48.4%)	0.001
Laboratory parameters					
Glucose	117.3±46.5	108.8±35.9	120.4±48.5	119.5±50.5	0.412
Hb A1c(%)	6.2±0.9	6.0±0.5	6.3±0.9	6.3±1.0	0.108
Serum creatinine. mg/dL	1.0±0.3	0.9±0.4	1.0±0.3	1.0±0.3	0.166
Glomerular filtration rate. mL/min	66.1±10.2	67.6±9.2	65.6±10.7	65.7±10.1	0.567
Triglycerides. mg/dL	157.2±179.7	116.9±47.3	150.1±82.9	192.7±286.9	0.100
Cholesterol. mg/dL	184.4±47.7	206.4±40.4	178.6±44.2	177.1±52.4	0.003
HDL cholesterol. mg/dL	49.3±17.5	63.9±22.1	45.3±12.3	44.6±14.2	0.001
LDL cholesterol. mg/dL	112.6±37.7	121.6±32.2	109.7±33.1	110.3±45.4	0.221
C-reactive protein. mg/L	5.2±11.2	3.3±4.6	5.7±13.9	5.7±10.4	0.483
Leucocytes. 109/L	7.3±2.1	6.9±2.3	7.4±2.1	7.3±2.1	0.413
CD marker					
Concentration of AnnV+ MV/µl	738.0±1866.7	557.8 ±887.6	716.7±1300.7	883.6±2748.9	0.683

*p values reflect the Pearson chi-square test results for categorical variables and analysis of variance for continuous variables. Continuous variables are presented as the mean ± SD, and categorical variables are presented as the percentage of patients. NCAD, non-coronary artery disease; Stable CAD, stable coronary artery disease; ACS, acute coronary syndrome; MI, myocardial infarction; PCI, percutaneous coronary intervention; ACE, angiotensin-converting enzyme; LDL, low-density lipoprotein; HDL, high-density lipoprotein; MV, microvesicle. Chronic kidney disease was defined as a glomerular filtration rate <60 mL/min.

3.3 miR selection and detection in circulating MV

Circulating miRs protected by circulating MV regulate the progression of coronary artery disease(Boulanger, et al., 2017) and are associated with cardiovascular outcomes(Jansen, et al., 2014). However, the expression profile of MV-miRs in patients with or without CAD has not been systemically explored so far. Therefore, miR profile in isolated circulating MV from stable CAD (n=5) and ACS patients (n=5) were assessed using taqman miR array. Among the multiple differentially expressed miRs between stable CAD and ACS patients (Figure 2), 9 miRs with known regulatory roles in the development and progression of atherosclerosis and coronary artery disease were selected for prospective quantification in our validation cohort of 180 patients without CAD, stable CAD or ACS: miR-21(Thum, et al., 2008), miR-26(Jansen, et al., 2016), miR-92(Hinkel, et al., 2013), miR-126(Jansen, et al., 2013), miR-139(Voellenkle, et al., 2010), miR-199(Rane, et al., 2009) and miR-222(Jansen, et al., 2015), miR-let7(Yu, et al., 2011), miR-30(Chen, et al., 2014, Shen, et al., 2015).

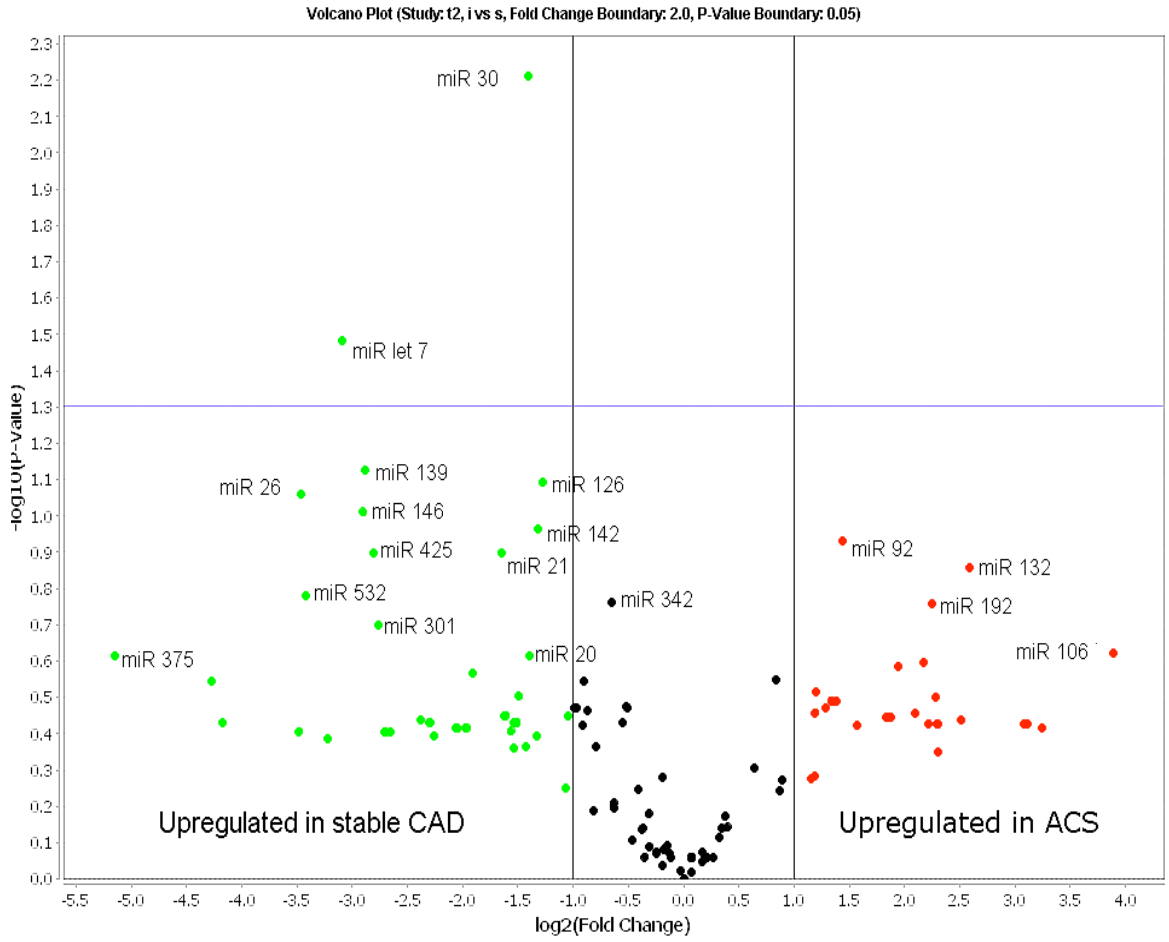

Fig. 2: MV-miRs screening

Volcano plot analysis showed miR profile in isolated circulating MV from stable CAD and ACS patients as determined TaqMan miR array (n=5). The horizontal line displays the border for significant regulation. Points above that line represent significantly regulated miRs (P<0.05(−log10)). MV, microvesicle.

Analysis of miR expression pattern in isolated MV from NCAD, stable CAD and ACS patients showed no difference regarding miR-21, miR-26, miR-126, miR-139, miR-199, miR-222, miR-let7 and miR-30. In contrast, miR-92 was significantly increased in stable CAD and ACS patients compared to NCAD patients (*P<0.05, Figure 3). Based on these observations, we sought to further characterize the role of MV-incorporated miR-92.

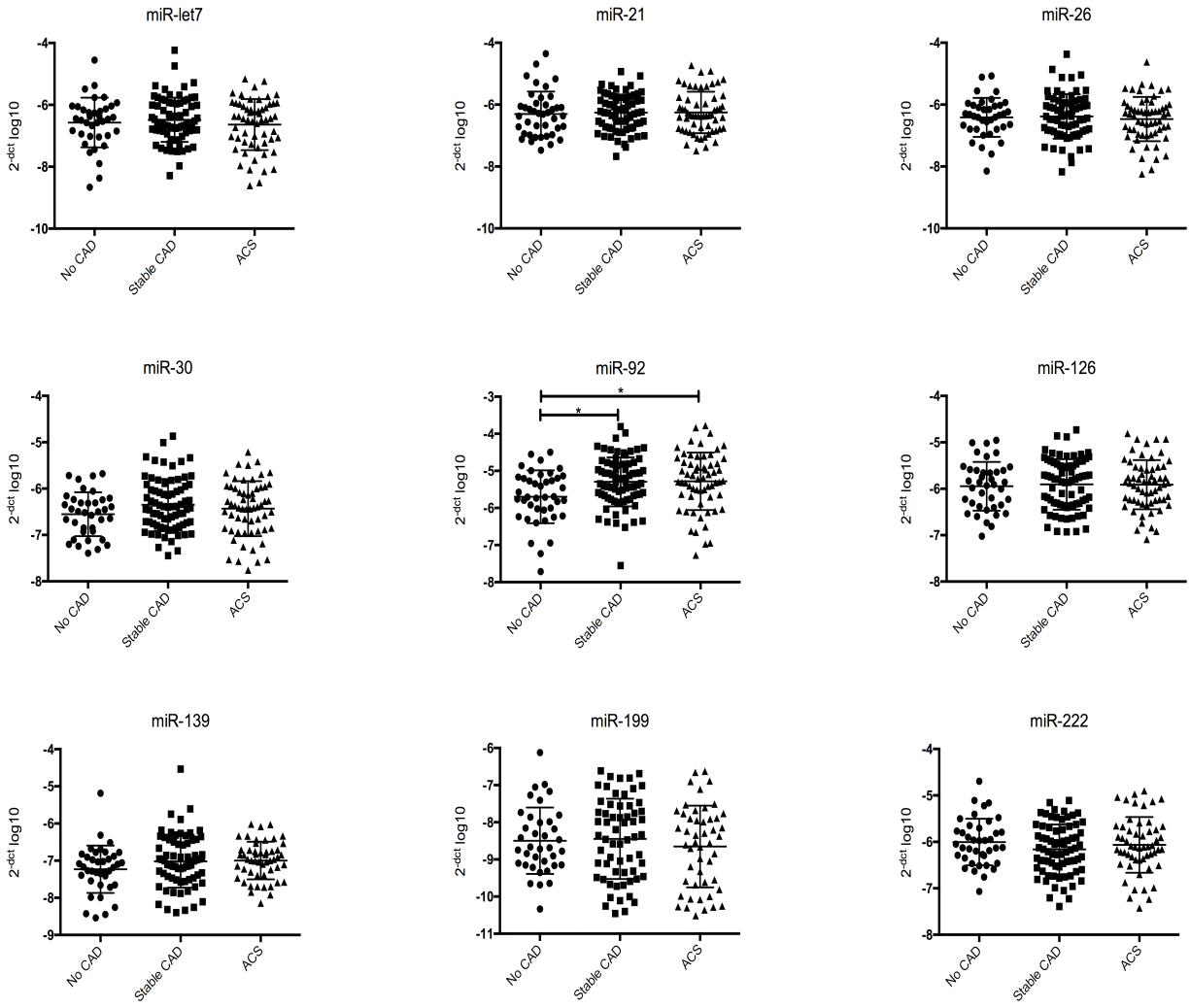

Fig. 3: miR expression analysis in patients with or without CAD

miR expression was analyzed in circulating MV in patients with angiographically excluded CAD (No CAD, n=41), stable CAD (n=77) and ACS (n=62) patients. Values were normalized to cel-miR-39 and were expressed as $2^{-[CT(miR)-CT(cel\text{-}miR\text{-}39)]}$ log10. Data are presented as mean±SD (*P<0.05, by 1-way ANOVA with Bonferroni's multiple comparisons test). MiR indicates microRNA; MV, microvesicle; CAD, coronary artery disease; ACS, acute coronary syndrome.

Comorbidities such as hypertension and diabetes or medication potentially affect circulating MV-bound miRs levels. However, binary logistic regression demonstrated that

higher or lower levels of miR-92 were not associated with any comorbidities (Table 2). Furthermore, miR-92 levels were independent of any drug therapy (Table 2).

Tab. 2: Association of the level of miR-92 with baseline characteristics

	Exp(B) (95% CI)	P Value
Age	1.020(0.982 to 1.060)	0.304
Male sex	1.627 (0.651 to 4.069)	0.298
Body mass index	0.924 (0.845 to 1.010)	0.080
Arterial hypertension	0.762 (0.296 to 1.963)	0.574
Hyperlipoproteinemia	0.824 (0.374 to 1.813)	0.630
Diabetes	1.859 (0.991 to 3.488)	0.053
Family history of CAD	0.780 (0.309 to 1.966)	0.598
Smoking	1.537 (0.616 to 3.832)	0.357
History of myocardial infarction	0.748 (0.279 to 2.002)	0.563
Chronic kidney disease	0.430 (0.279 to 5.498)	0.516
Number of diseased vessels	0.785(0.608 to 1.014)	0.064
Left ventricular ejection fraction	0.995 (0.963 to 2.002)	0.754
Previous PCI	0.560 (0.210 to 1.028)	0.247
Current PCI	0.815 (0.327 to 2.030)	0.661
Angiotensin Converting Enzyme inhibitors (ACEI)	0.915 (0.275 to 3.047)	0.885
Angiotensin receptor blockers (ARB)	0.658 (0.171 to 2.530)	0.542
Beta blockers	1.907 (0.600 to 6.063)	0.274
Calcium channel blockers (CCB)	0.828 (0.282 to 2.430)	0.732
Diuretics	1.002 (0.417 to 2.409)	0.997
Statins	1.229 (0.329 to 4.595)	0.759
Nitrates	8.061 (0.719 to 90.369)	0.091
Aspirin	1.160 (0.295 to 4.566)	0.832

The coefficient of the continuous variables was relative to 1-U differences. Binary logistic regression according to the median of miR-92 level. ACE indicates angiotensinconverting enzyme; CAD, coronary artery disease; Exp(B), exponentiation of the B coefficient; miR, microRNA.

3.4 miR-92 expression in MV, exosomes and vesicle-free plasma

Circulating miRs in plasma can be transported within extracellular vesicles (exosomes, MV, apoptotic bodies) or bound to proteins (high-density lipoprotein, Ago-2). Both routes provide remarkable stability and resistance to degradation from endogenous RNase activity. Next, we aimed to explore the plasma compartments (exosomes, MV, vesicle-free plasma) in which miR-92 is mainly expressed. Consequently, MV, exosomes, and vesicle-free plasma were collected by series of centrifugation steps, and miR-92 was analyzed in the sub-compartments of 10 patients with stable CAD. Electron microscopy confirmed a proper isolation of exosomes and MV according to the used protocol (Figure 4A). miR-92 was detectable mainly in MV or vesicle-free plasma (Figure 4B).

Because circulating MV compose different subspecies of membrane particles released from endothelium and blood cells, we sorted endothelial-, platelet-, and other cell-derived MV using flow cytometer to explore the cellular origins of MV-bound miR-92 as previously described(Jansen, et al., 2016, Jansen, et al., 2014). Overall, miR-92 showed the highest expression in $CD31^{+}/CD42b^{-}$ endothelial cell-derived MV (EMV), compared to $CD31^{+}/CD42b^{+}$ platelet-derived MV (PMV) and $CD31^{-}/CD42b^{-}$ MV (Figure 4C). Similarly, in vitro, miR-92 also showed the highest expression in EMV, compared to PMV and monocyte-derived MV (MMV, Figure 4D). These results suggest that miR-92 is selectively packaged into EMV in patients and in vitro.

A

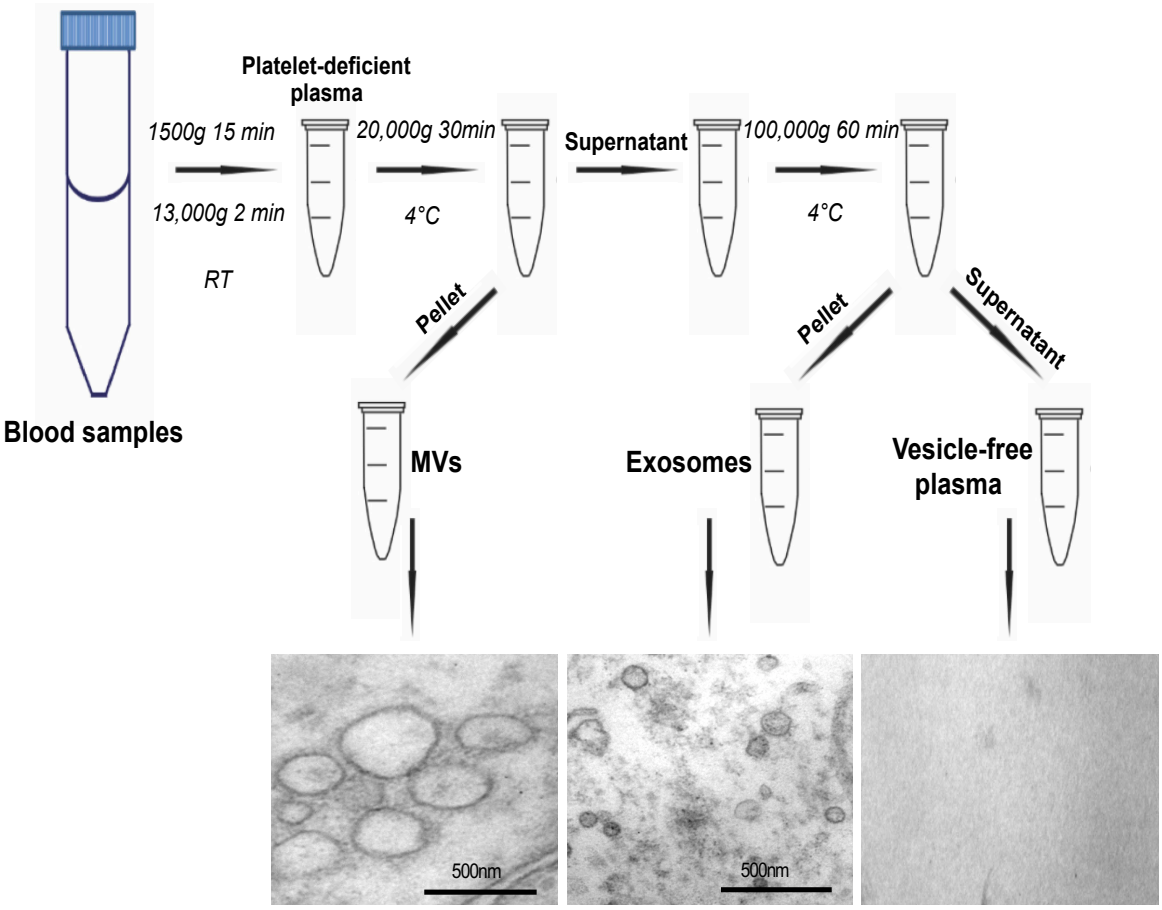
Blood samples
Platelet-deficient plasma
1500g 15 min
13,000g 2 min
RT
20,000g 30min
4°C
Pellet
MVs
Supernatant
100,000g 60 min
4°C
Pellet
Exosomes
Supernatant
Vesicle-free plasma
500nm
500nm
20,000g pellet
100,000g pellet
supernatant

B

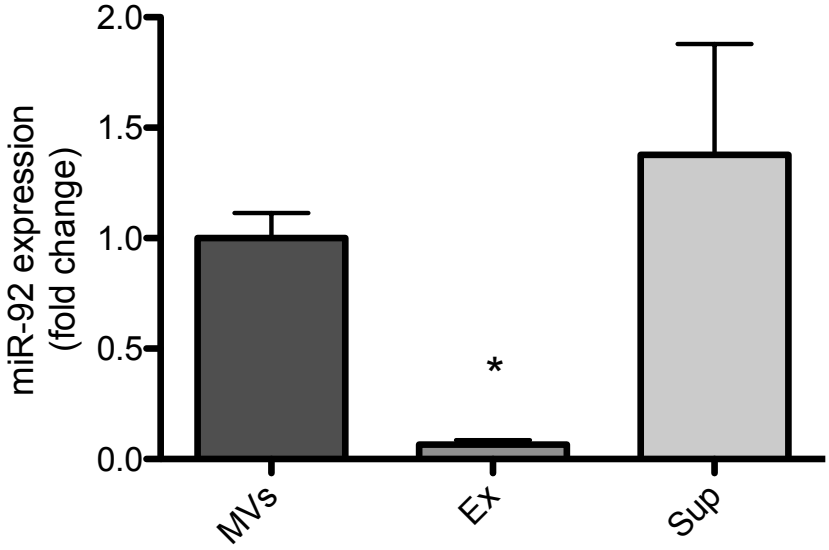
2.0
1.5
1.0
0.5
0.0
miR-92 expression
(fold change)
*
MVs
Ex
Sup

C

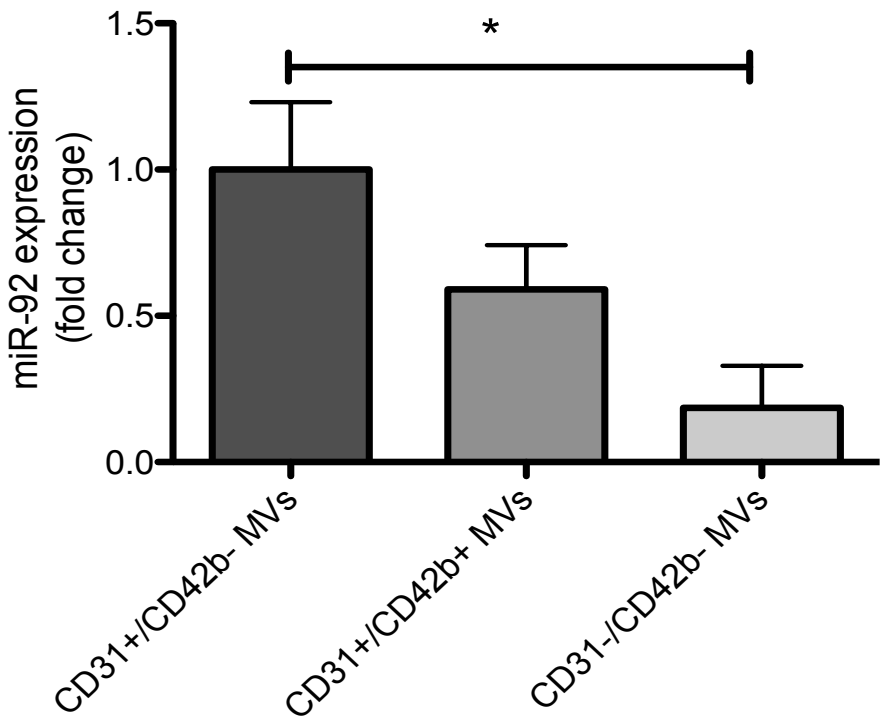
1.5
1.0
0.5
0.0
miR-92 expression
(fold change)
*
CD31+/CD42b- MVs
CD31+/CD42b+ MVs
CD31-/CD42b- MVs

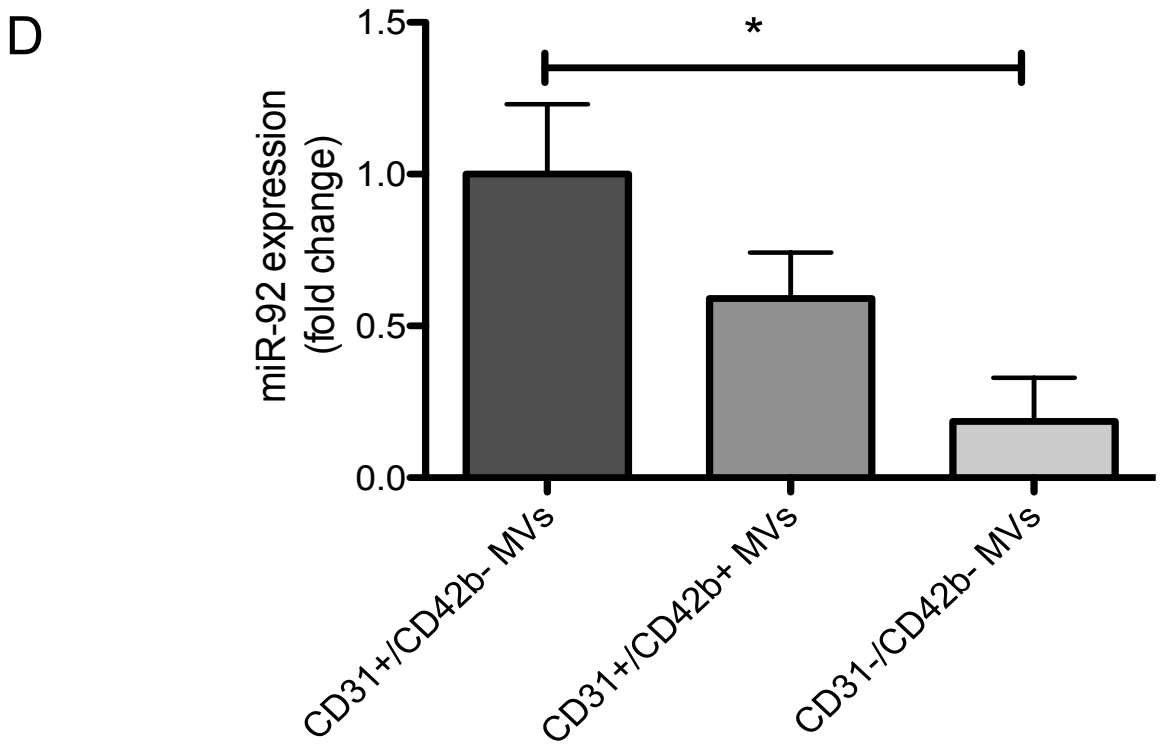

Fig. 4: miR-92 expression in plasma subpopulations

(A) Expression of miR-92 in plasma compartments. MV and exosomes were isolated using 20,000g and 100,000g centrifugation. Characterization of MV, exosomes and the last supernatant were performed using electron microscopy. Magnification ×46,000. (B) MiR-92 was quantified in MV, exosomes, and vesicles-free supernatant by real-time PCR (*P<0.05, n=6, by 1-way ANOVA with Bonferroni's correction for multiple comparisons test). Cel-miR-39 was used as control. (C) Endothelial cell–derived (CD31+/CD42b-), platelet-derived (CD31+/CD42b+), and other cell–derived MV (CD31-/CD42b-) were collected from 10 plasma samples of CAD patients, and miR-92 expression was analyzed in MV subspecies in vivo by real-time PCR (*P<0.05, n=10, by 1-way ANOVA with Bonferroni's correction for multiple comparisons test). Cel-miR-39 was used as control. (D) EMV, PMV and MMV were isolated from corresponding cells and miR-92 expression was analyzed in MV subspecies in vitro by real-time PCR (*P<0.05, **P<0.01, n=3-5, by 1-way ANOVA with Bonferroni's correction for multiple comparisons test). RNU6B was used as an endogenous control. MV indicates microvesicle; CAD, coronary artery disease; Ex, exosomes; Sup, supernatant. EMV, endothelial cell–derived microvesicle; PMV, platelet-derived microvesicle; MMV, monocyte-derived microvesicle.

3.5 oxLDL stimulation in vitro increases EMV-incorporated miR-92 expression in a STAT3-dependent mechanism

As MV-incorporated miR-92 was significantly increased in CAD patients and endothelial cell-derived MV were shown to be the major source of miR-92-containing MV, we next explored the effect of atherosclerotic conditions in vitro on miRs expression in ECs and EMV. As an independent risk factor of atherosclerosis, several lines of evidence indicate that low-density lipoprotein (LDL) and especially it's oxidized form (oxLDL) play a key role in endothelial dysfunction and atherogenesis(Chen, et al., 2002, Pirillo, et al., 2013). To explore whether oxLDL might affect miRs levels in ECs and EMV, ECs were incubated with oxLDL for 24 hours and EMV were isolated subsequently. Real-time PCR analysis of the nine selected miRs revealed that mainly miR-92, but also miR-222, miR-26 and miR-let7 were selectively sorted into EMV after oxLDL stimulation (Figure 5A)

To further investigate the link between oxLDL and miR-92, we quantified miR-92 expression in ECs and EMV after stimulation with different oxLDL concentrations. OxLDL stimulation significantly increased miR-92 expression both in EMV and ECs in a dose-dependent effect (Figure 5B and 5C). In summary, our findings indicate that oxLDL induces cellular miR-92 expression and promotes the packaging of miR-92 from ECs into EMV.

Signal transducer and activator of transcription 3 (STAT3) is a transcription factor that controls a battery of genes involved in the regulation of a variety of biological processes. Previous studies identified a highly conserved STAT3-binding site in the promoter of the EFCAB12 gene, which encodes the entire miR-17-92 cluster(Brock, et al., 2011). To examine the direct effect of STAT3 activation on miR-92 expression in ECs and EMV, we selectively blocked STAT3 activity using a STAT3 inhibitor in ECs and EC-derived MV. miR-92 expression analysis revealed that STAT3 inhibition significantly reduced miR-92 expression in ECs and EMV in a dose-dependent mechanism (Figure 5D and 5E), highlighting a regulatory role of STAT3 in endothelial miR-92 expression and MV packaging.

A

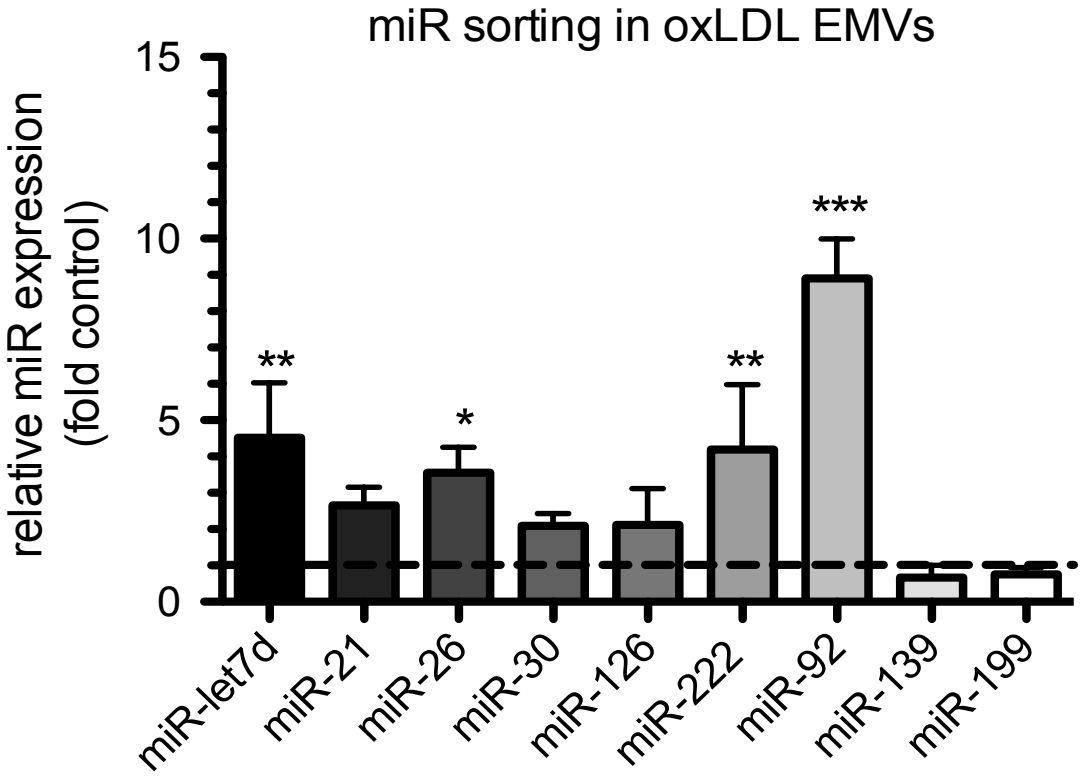
miR sorting in oxLDL EMVs
relative miR expression
(fold control)
15
10
5
0
**
*
**
***
miR-let7d
miR-21
miR-26
miR-30
miR-126
miR-222
miR-92
miR-139
miR-199

B

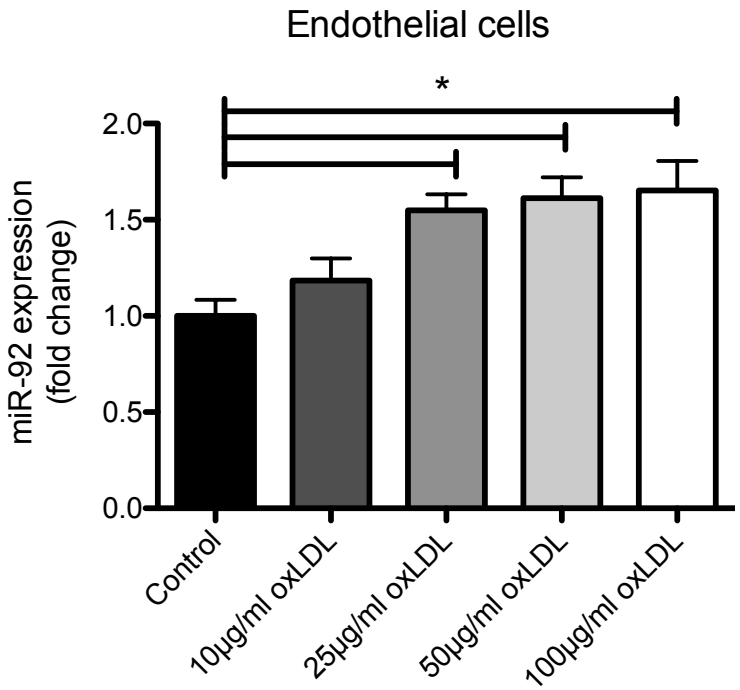
Endothelial cells
*
miR-92 expression (fold change)
2.0
1.5
1.0
0.5
0.0
Control
10µg/ml oxLDL
25µg/ml oxLDL
50µg/ml oxLDL
100µg/ml oxLDL

C

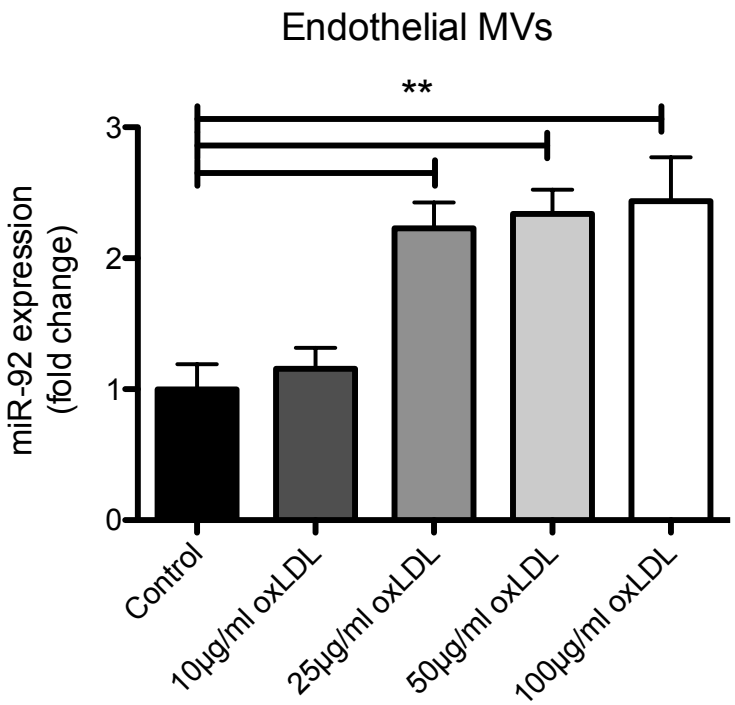
Endothelial MVs
**
miR-92 expression (fold change)
3
2
1
0
Control
10µg/ml oxLDL
25µg/ml oxLDL
50µg/ml oxLDL
100µg/ml oxLDL

D

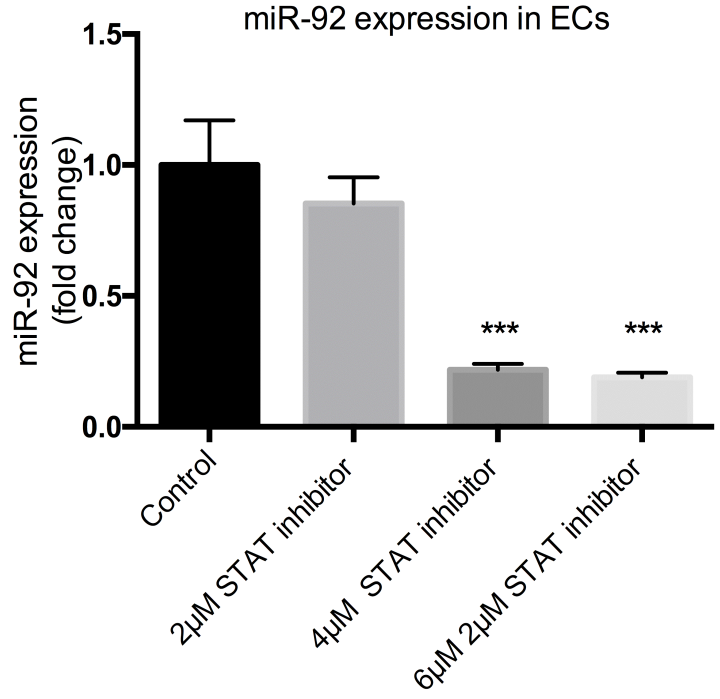
miR-92 expression in ECs
miR-92 expression (fold change)
1.5
1.0
0.5
0.0
***
***
Control
2μM STAT inhibitor
4μM STAT inhibitor
6μM 2μM STAT inhibitor

E

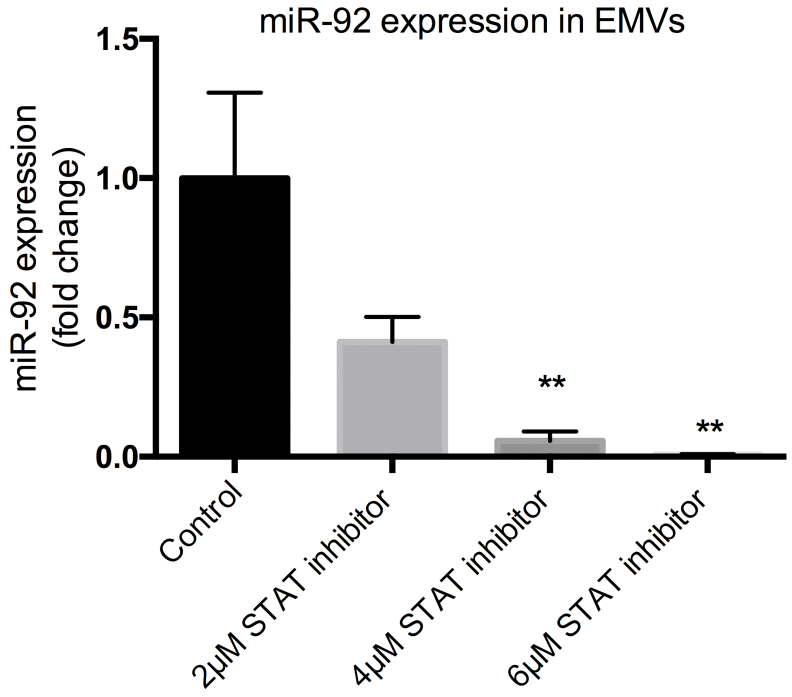
miR-92 expression in EMVs
miR-92 expression (fold change)
1.5
1.0
0.5
0.0
**
**
Control
2μM STAT inhibitor
4μM STAT inhibitor
6μM STAT inhibitor

Fig. 5: OxLDL increases miR-92 expression in ECs and EMV

(A) miR-let7, miR-21, miR-26, miR-30, miR-126, miR-222, miR-92, miR-21 and miR-199 ere analyzed in oxLDL EMVs by real-time PCR (*P<0.05, **P<0.01, ***P<0.001, n=5, by 1-way ANOVA with Bonferroni's correction for multiple comparisons test). Non-treated EMV served as control. (B, C) MiR-92 was analyzed in ECs and EMVs after stimulation with different oxLDL concentrations by real-time PCR (*P<0.05, **P<0.01, n=5, by 1-way ANOVA with Bonferroni's correction for multiple comparisons test). (D, E) MiR-92 was measured in ECs and EMVs after stimulation with different concentrations of STAT3 inhibitor by real-time PCR (***P<0.001, **P<0.01, n=5-6, by 1-way ANOVA with Bonferroni's correction for multiple comparisons test). RNU6B was used as an endogenous control in real-time PCR. OxLDL indicates oxidized low-density lipoprotein; EMVs indicates endothelial cell-derived microvesicles; ECs, endothelial cells; STAT3, signal transducer and activator of transcription 3.

3.6 miR-92 in EMV regulates target ECs function

Increasing evidence suggests that MV emerge as major transport vehicles for miRs and that the effects of MV depend on the MV-containing miRs expression. To study the biological function of incorporated miR-92 in EMV, we investigated first whether MV miR-92 can be internalized by recipient cells. To visualize the transport of MV miR-92 derived from ECs into recipient cells, we transfected donor ECs with Cy3 labeling miR-92 (Cy3-miR-92) and isolated Cy3-miR-92 containing EMV were isolated from donor ECs. Then the EMV were labeled with PKH67. After incubation with labeled EMV, co-localization of Cy3-miR-92 (red) and PKH67 (green) was observed in most recipient cells by using fluorescent microscopy (Figure 6A). Furthermore, copy number assays using real-time PCR confirmed an efficient transfer of miR-92 into recipient cells via EMV (Figure 6B)

A

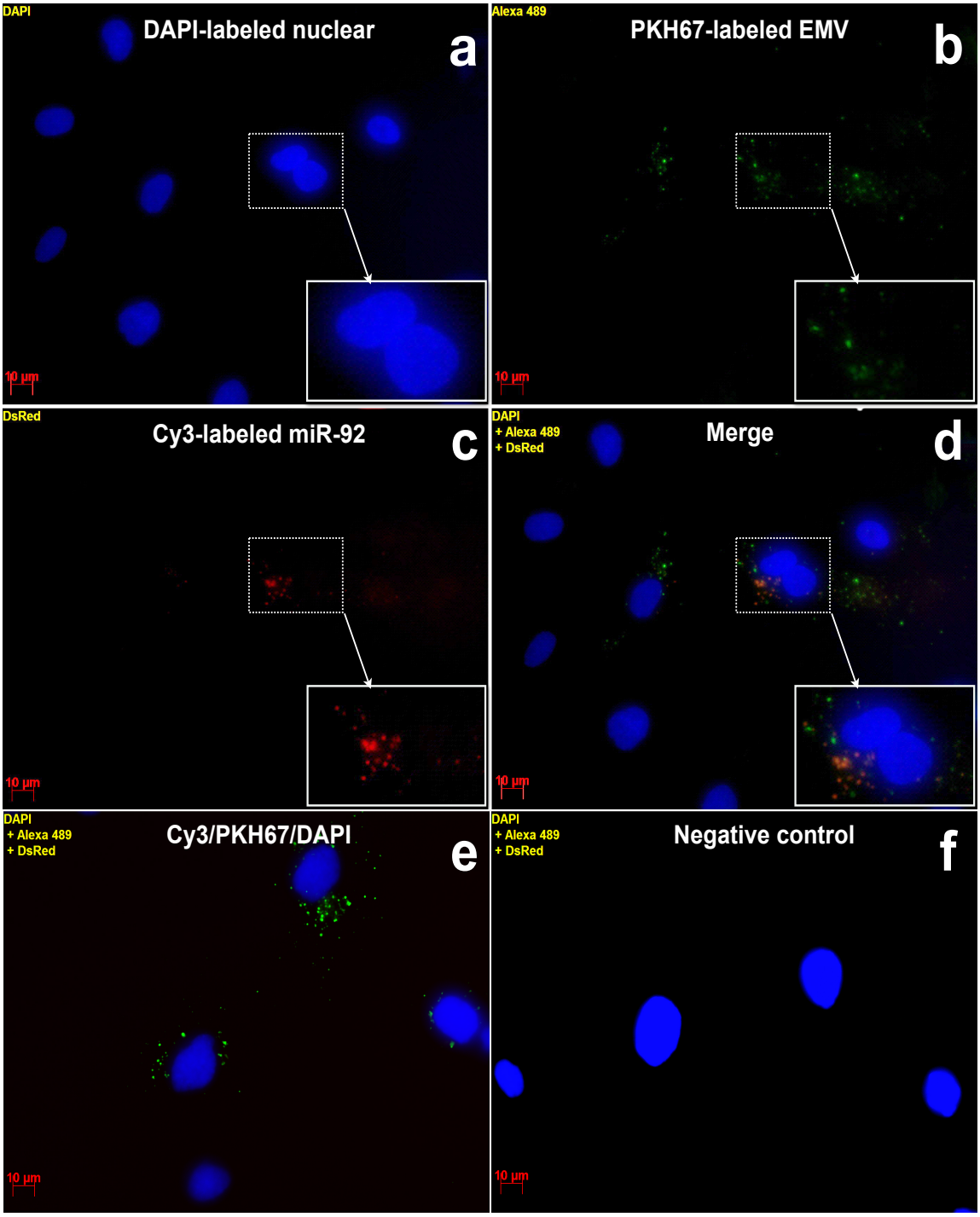
DAPI
DAPI-labeled nuclear
a
10 μm
Alexa 489
PKH67-labeled EMV
b
10 μm
DsRed
Cy3-labeled miR-92
c
10 μm
DAPI
+ Alexa 489
+ DsRed
Merge
d
10 μm
DAPI
+ Alexa 489
+ DsRed
Cy3/PKH67/DAPI
e
10 μm
DAPI
+ Alexa 489
+ DsRed
Negative control
f
10 μm

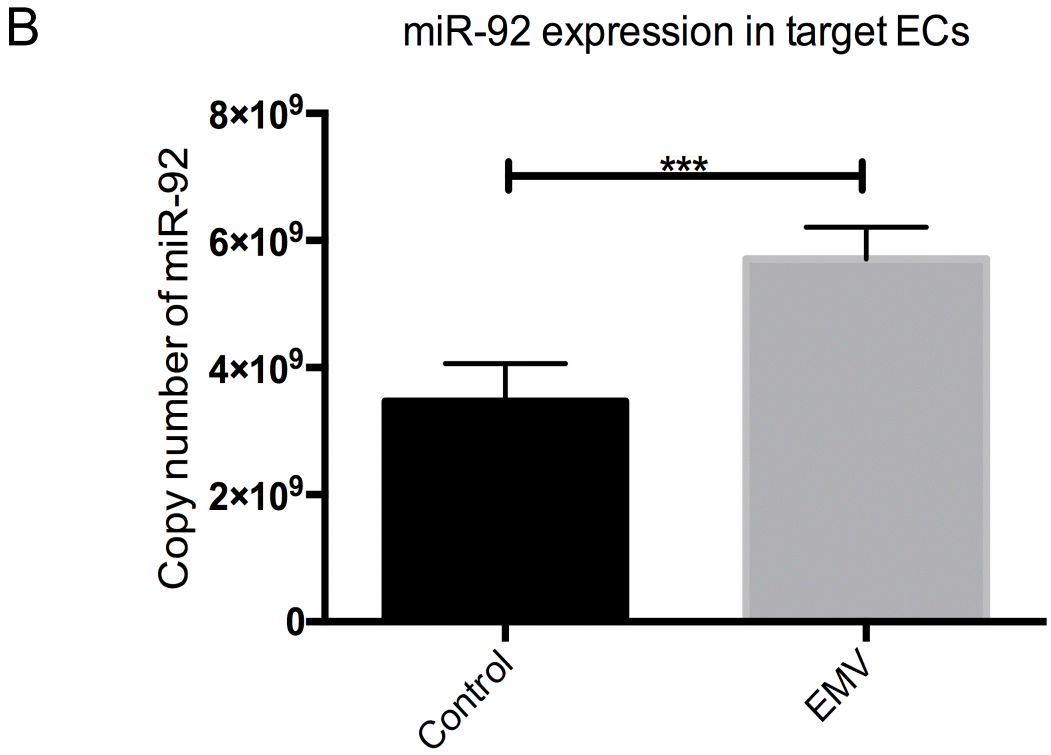

Fig. 6: EMV-incorporated miR-92 is transferred into recipient ECs

(A) Cy3-labeled miR-92 was transfected into ECs and EMV were derived, then EMV labeled with PKH67. PKH67-labelled EMV that contained Cy3-labeled miR-92 were cultured with recipient ECs for 6 hours. Cells nuclei were stained with DAPI and pictures were taken. Bars: 10 μm. a) Nuclei were stained with DAPI (blue). b) EMV were labeled with PKH67 (green) c) Red showed Cy3-labeled miR-92. d) The Cy3-miR-92 signals co-localized with PKH67. e) As a negative control for detection of the Cy3 signals, ECs were cultured with non-labeled miR-92 within EMV. f) As a negative control for PKH67, ECs were cultured with unlabeled EMV. (B) MiR-92 expression in target ECs that were treated with EMV or vehicle was quantified using copy number analysis (***P<0.001, n=4, by student t test). EMV indicates endothelial cell-derived microvesicle; Cy3, cyanine 3; EC, endothelial cell; DAPI, 4′,6-diamidino-2-phenylindole.

Next, we aimed to explore the biological function of EMV-incorporated miR-92. As miR-92 has been shown to be a major regulator of angiogenesis(Zhang, et al., 2014), we investigated whether miR-92 in EMV can functionally regulate target EC migration, proliferation and tube formation. Therefore, miR-92 inhibitor was used to inhibit miR-92 expression in EC and EC-derived EMV to generate $EMV^{miR\text{-}92\text{-}downregulated}$ and the corresponding control group ($EMV^{mock\text{-}transfected}$). Efficient miR-92 downregulation in EMV parent cells and EMV by using inhibitor was confirmed by real-time PCR (Figure 7). Copy number experiments revealed that downregulation of miR-92 in EMV resulted in a reduced transfer of miR-92 in recipient cells (Figure 8). Treatment of target ECs with EMV promoted EC migration, proliferation and tube formation in vitro (Figure 9). Importantly, EMV-mediated effects on recipient ECs were abolished using $EMV^{miR\text{-}92\text{-}downregulated}$, indicating that miR-92 in EMV functionally regulates target ECs function and phenotype by promoting angiogenic processes (Figure 9).

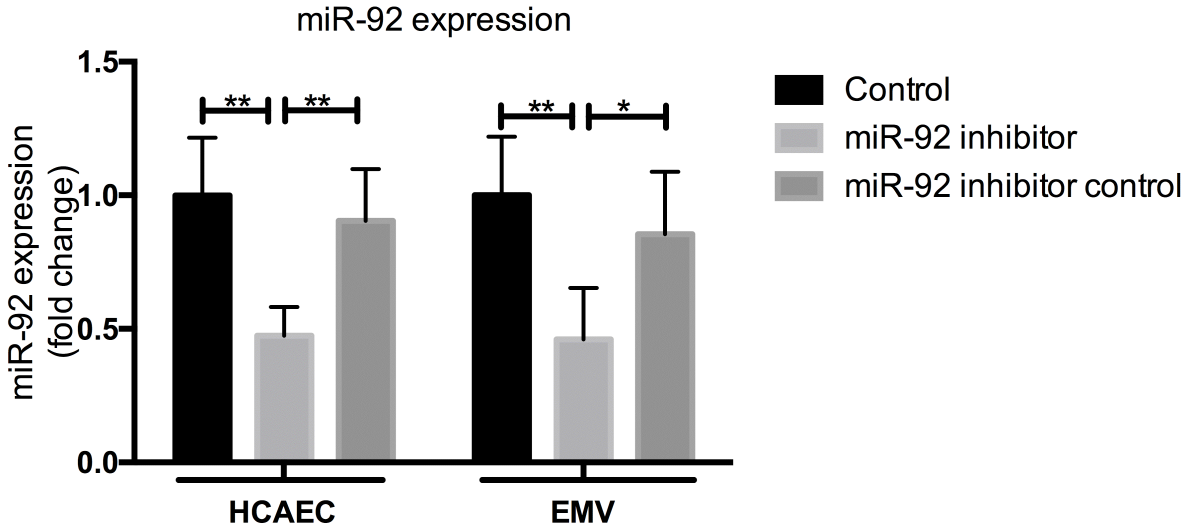

Fig. 7: miR-92 expression in EMV and EMV donor cells

ECs were transfected with miR-92 inhibitor or the corresponding mock and then subjected to basal media to generate EMV. MiR-92 expression was analyzed in EMV and EMV donor cells by real-time PCR

(*P<0.05, **P<0.01, n=5, by 1-way ANOVA with Bonferroni's multiple comparisons test). RNU6B was used as an endogenous control. EMV indicates endothelial cell-derived microvesicle; ECs, endothelial cells.

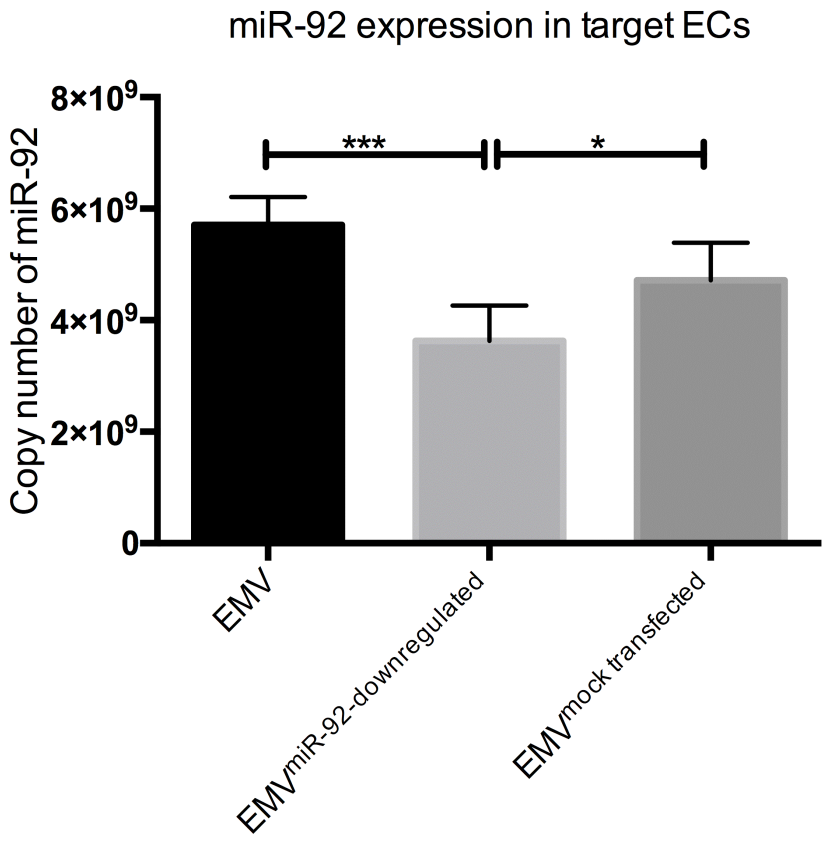

Fig. 8: EMV-incorporated miR-92 is transferred into target ECs

miR-92 expression in recipient ECs that were treated with EMV, $EMV^{miR\text{-}92\text{-}downregulated}$, $EMV^{mock\text{-}transfected}$ by copy number analysis (*P<0.05, ***P <0.001, n=4, by 1-way ANOVA with Bonferroni's multiple comparisons test). EC indicates endothelial cell; EMV, endothelial cell-derived microvesicle.

A

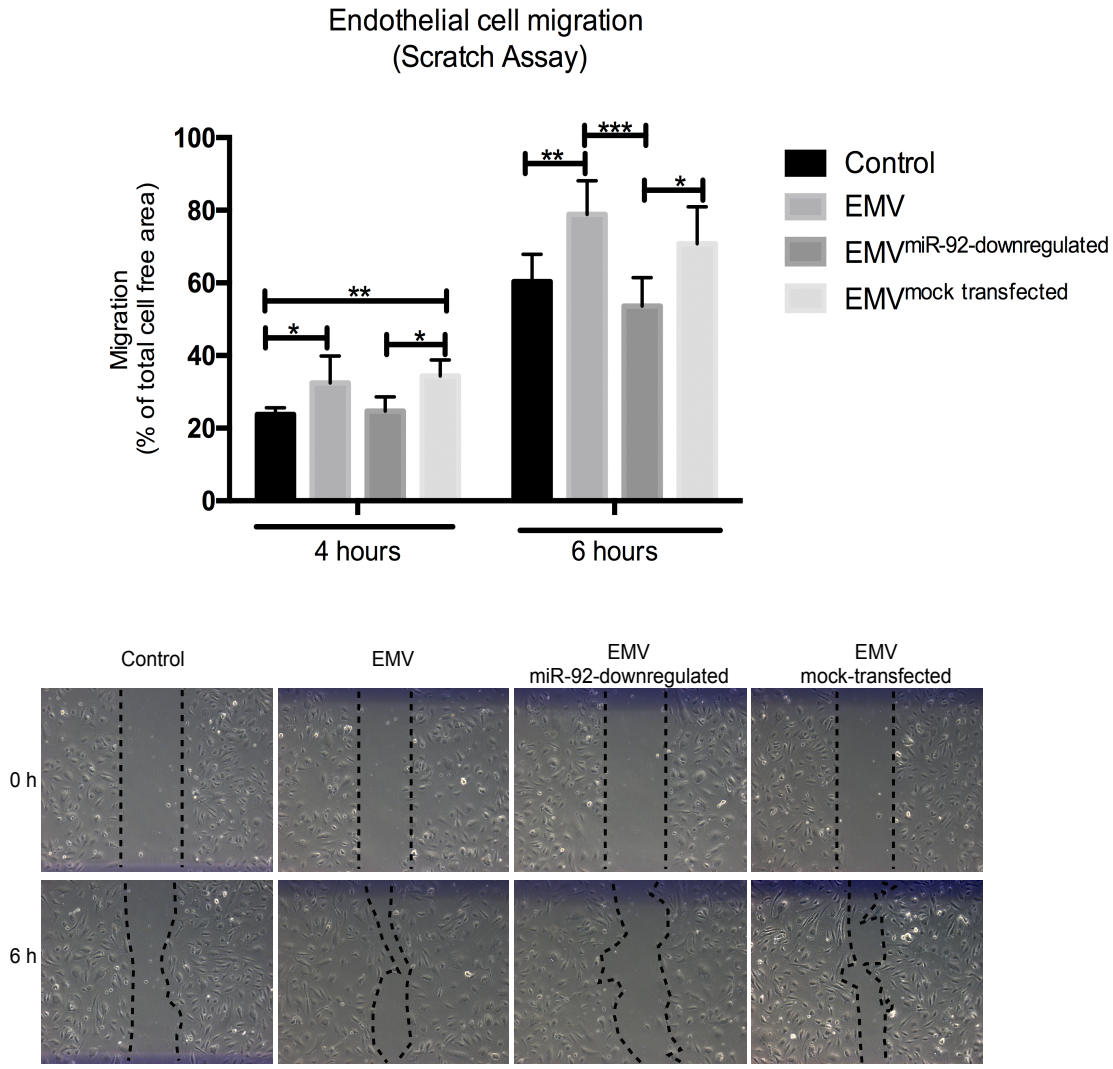
Endothelial cell migration
(Scratch Assay)
Migration
(% of total cell free area)
100
80
60
40
20
0
**
*
*
**
***
*
4 hours
6 hours
Control
EMV
EMV miR-92-downregulated
EMV mock transfected
Control
EMV
EMV
miR-92-downregulated
EMV
mock-transfected
0 h
6 h

B

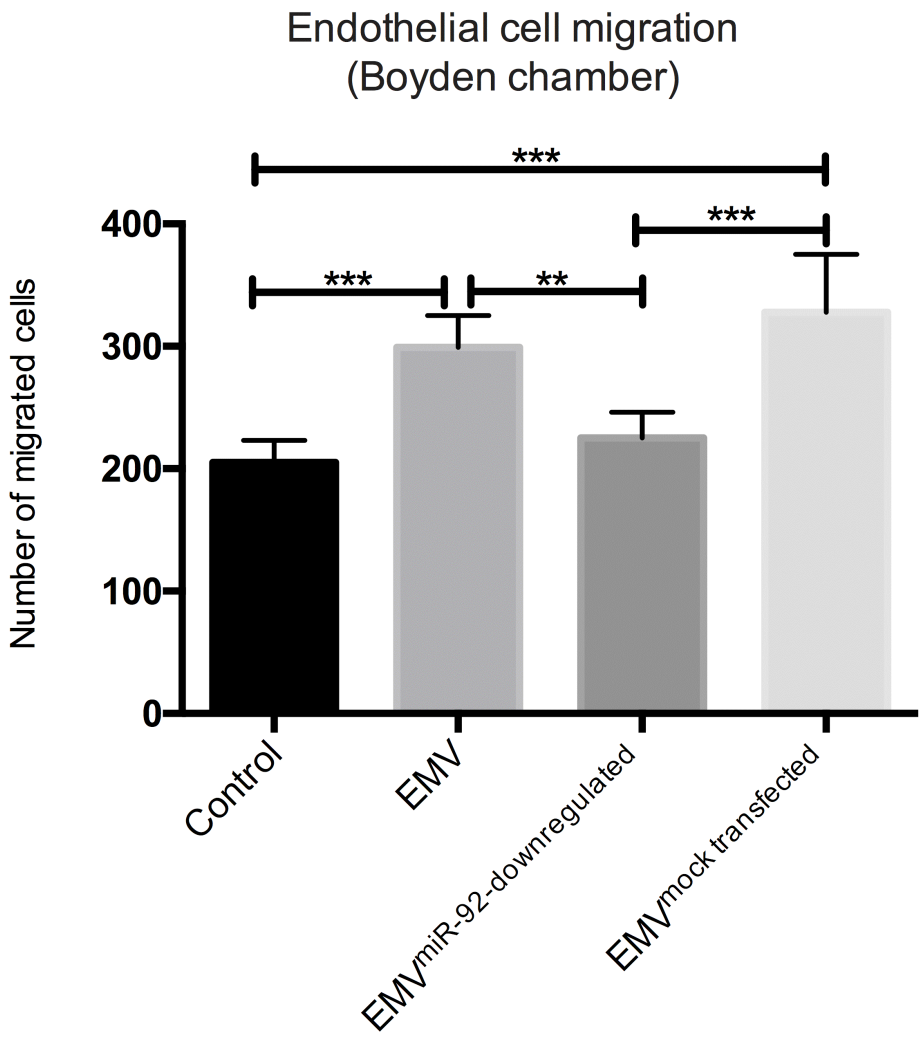
Endothelial cell migration
(Boyden chamber)
Number of migrated cells
400
300
200
100
0
***
***
***
**
Control
EMV
EMVmiR-92-downregulated
EMVmock transfected

C

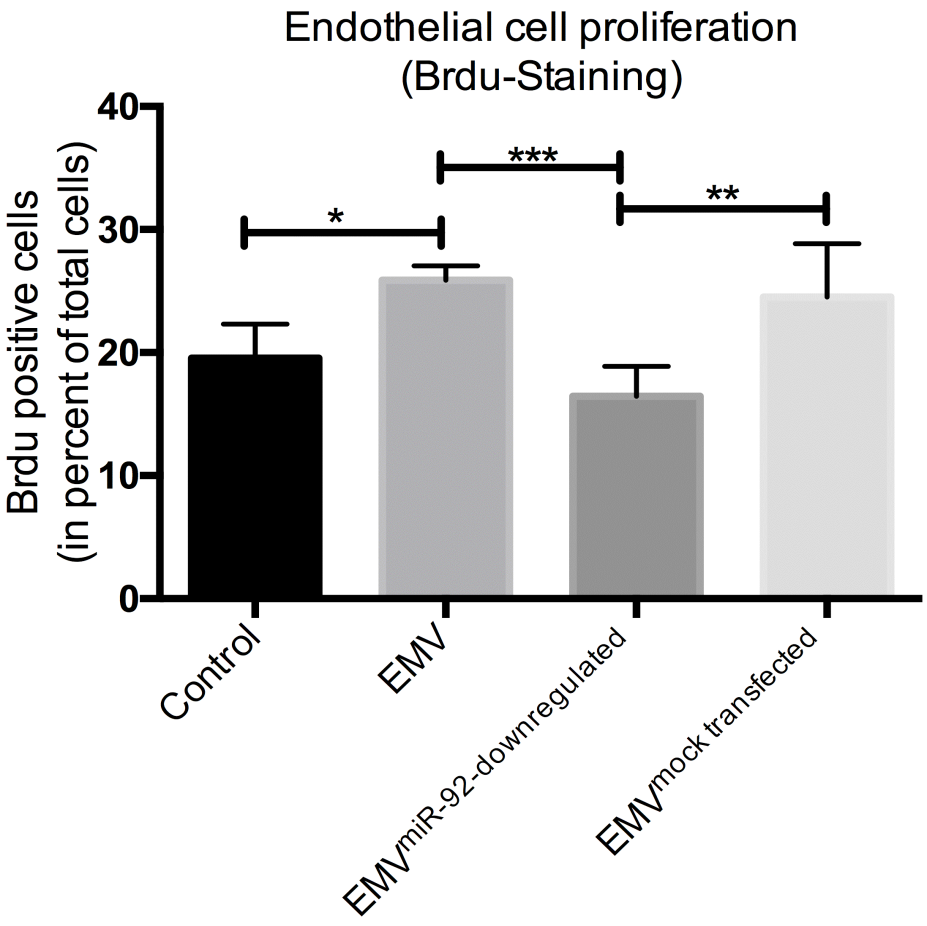
Endothelial cell proliferation
(Brdu-Staining)
Brdu positive cells
(in percent of total cells)
40
30
20
10
0
*
***
**
Control
EMV
EMVmiR-92-downregulated
EMVmock transfected

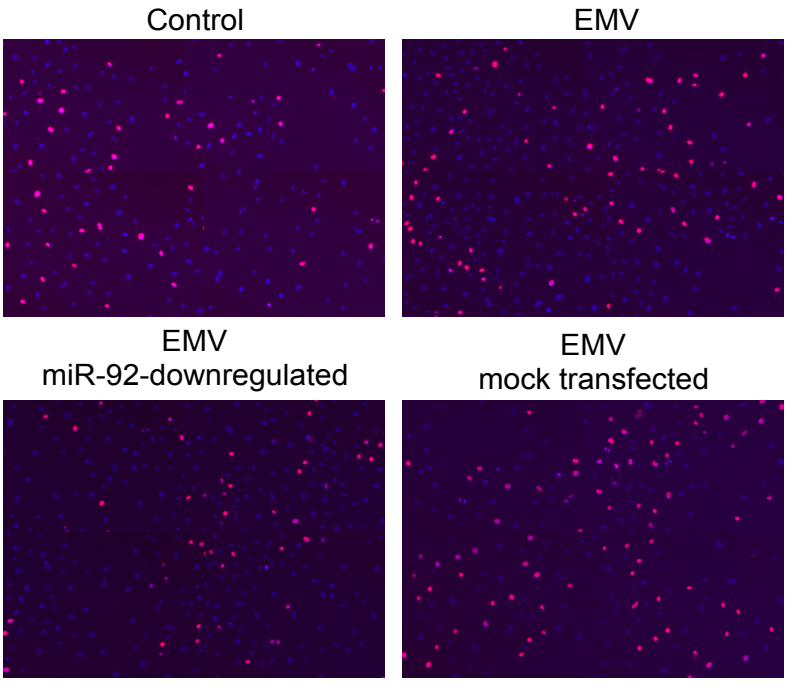
Control
EMV
EMV
miR-92-downregulated
EMV
mock transfected

D

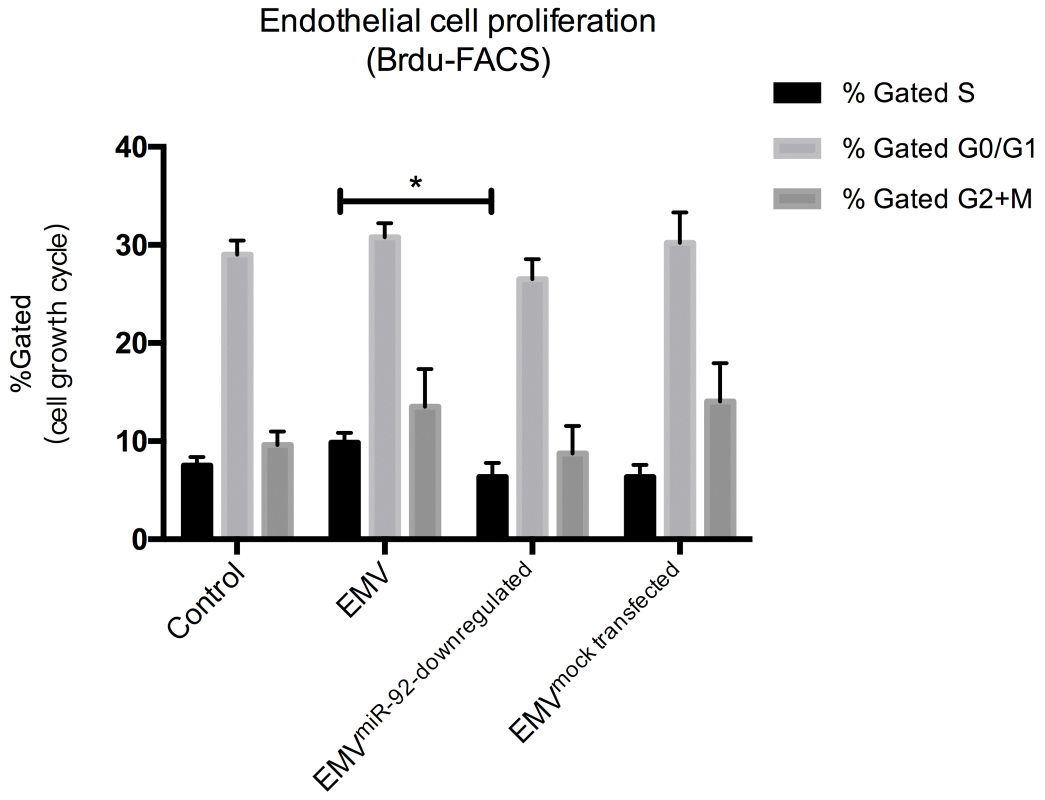
Endothelial cell proliferation
(Brdu-FACS)
% Gated S
% Gated G0/G1
% Gated G2+M
%Gated
(cell growth cycle)
40
30
20
10
0
*
Control
EMV
EMVmiR-92-downregulated
EMVmock transfected

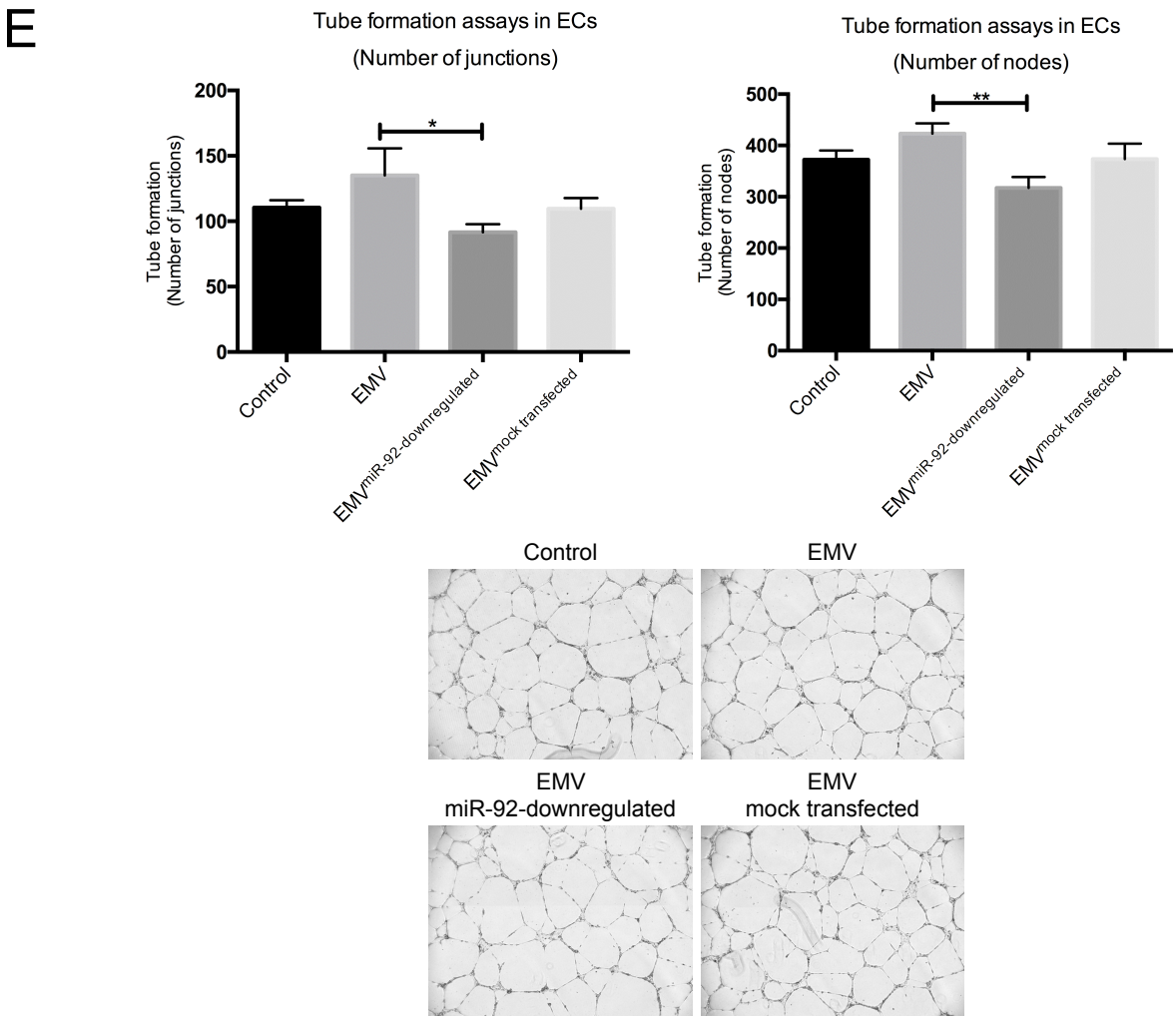

Fig. 9: miR-92 regulates EC migration, proliferation and angiogenesis via EMV

$EMV^{miR\text{-}92\text{-}downregulated}$ and $EMV^{mock\text{-}transfected}$ was separately derived from miR-92 inhibitor–transfected and mock-transfected parent cells. ECs in basal media were co-incubated with EMV, $EMV^{miR\text{-}92\text{-}downregulated}$, $EMV^{mock\text{-}transfected}$ or vehicle. (A) Scratch migration assay was performed and representative images of cells migrating into the scratched region were shown. Quantitative analysis of migration was measured as a percentage of total cell-free area (*P<0.05, **P <0.01, ***P<0.001, n=6, by 1-way ANOVA with Bonferroni's multiple comparisons test). (B) Boyden chamber migration assay was performed using ECs. Data represent the numbers of migrated cells (**P<0.01, ***P<0.001, n=5, by 1-way ANOVA with Bonferroni's multiple comparisons test). (C) BrdU incorporation was determined by immunofluorescence (red). Nuclei were stained with DAPI (blue). The percentage of BrdU-positive cells was compared (*P<0.05, **P<0.01,

***P<0.001, n=5, by 1-way ANOVA with Bonferroni's multiple comparisons test). Magnification ×100. (D) The incorporation of BrdU was normally analyzed in flow cytometry by labelling with a conjugate anti-BrdU antibody (*P<0.05, n=3, by 1-way ANOVA with Bonferroni's multiple comparisons test). (E) Tube formation assays of ECs. Capillary tubes were photographed with microscope. Tube junctions and nodes were measured and quantitatively analyzed using Image-Pro Plus software ((*P<0.05, **P<0.01, n=3, by 1-way ANOVA with Bonferroni's multiple comparisons test). EMV indicates endothelial cell-derived microvesicle; EC, endothelial cell; BrdU, bromodeoxyuridine and DAPI, 4′,6-diamidino-2-phenylindole.

3.7 EMV-mediated transfer of functional miR-92 regulates angiogenesis in recipient ECs in a THBS1-dependent mechanism

Finally, we aimed to investigate the underlying mechanism of EMV-transferred miR-92 in the regulation of angiogenic functions in recipient ECs. RT² Profiler PCR array analysis was performed to measure the expression of 84 key genes involved in modulating the biological processes of angiogenesis. As miRs regulate cellular phenotype by downregulating target mRNAs, we focused on downregulated genes in recipient ECs after treatment with vehicle, EMV and $EMV^{miR\text{-}92\text{-}downregulated}$. Profiler PCR array results showed that 53 genes were downregulated by EMV compared to control treatment, and 40 genes were downregulated by EMV compared to $EMV^{miR\text{-}92\text{-}downregulated}$ treatment. The five most downregulated genes in EMV vs. control and EMV vs. $EMV^{miR\text{-}92\text{-}downregulated}$ were separately selected and further explored (Figure 10A-C). Among those, 3 genes were simultaneously downregulated in response to EMV treatment compared to control and $EMV^{miR\text{-}92\text{-}downregulated}$: Thrombospondin 1(THBS1), TEK Receptor Tyrosine Kinase (TEK) and Angiopoietin 1 (ANGPT1, Figure 10C). Single real-time PCR experiments showed that only THBS1, a known target of miR-92(Italiano, et al., 2012), was downregulated in target ECs by EMV in a miR-92-dependent manner (Figure 10D-E). Furthermore, western blot experiments confirmed a miR-92–dependent downregulation of THBS1 expression in target ECs after EMV treatment (Figure 10F). These findings are consistent with the initial array results showing no change of THBS1 expression in target ECs after treatment with $EMV^{miR\text{-}92\text{-}downregulated}$ compared to control. Given the known evidence of THBS1 as a negative regulator of EC migration and proliferation(García-

Conesa, et al., 2009), further experiments were performed to evaluate whether miR-92 in EMV can inhibit THBS1 expression in target ECs and thereby promote EC migration and proliferation. Therefore, ECs were transfected with small interfering RNA against THBS1 or scrambled small interfering RNA (control small interfering RNA). Efficient THBS1 downregulation in target cells by using interfering RNA was confirmed by real-time PCR (Figure 11). Downregulation of THBS1 significantly increased EC migration and proliferation, confirming that THBS1 as a negative regulator of ECs migration and proliferation (Figure 12).

A

Scatter Plot
EMV vs. Control

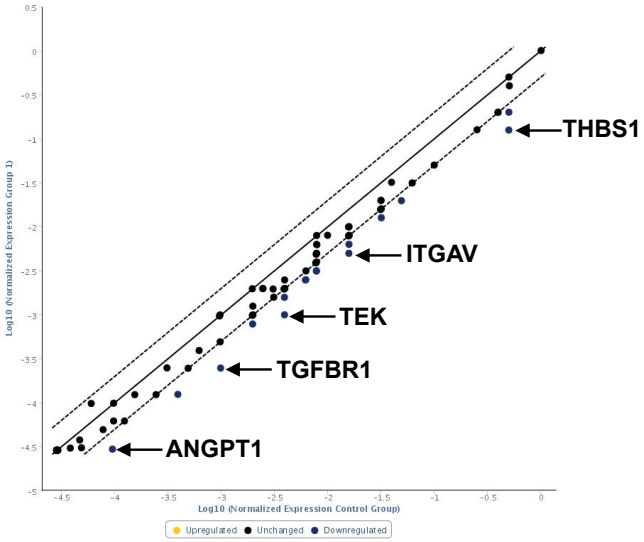

B

Scatter Plot
EMV vs. EMV$^{miR\text{-}92\text{-}downregulated}$

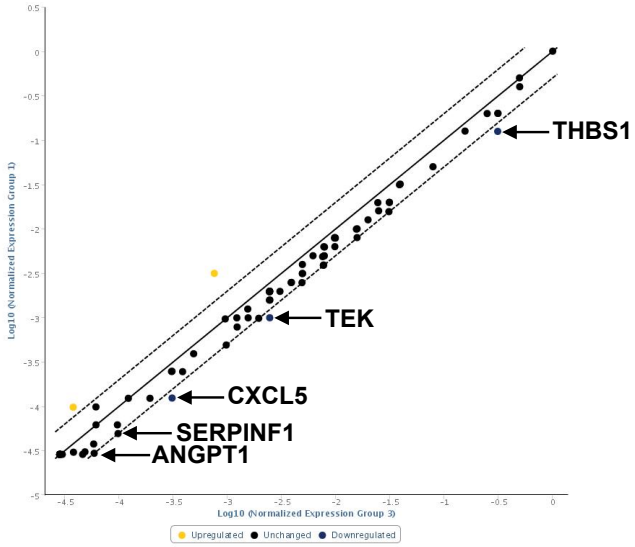

C

Top 5 downregulated genes in target ECs

EMV vs. Control		EMV vs. EMV$^{miR\text{-}92\text{-}downregulated}$	
Gene	Fold change	Gene	Fold change
TGFBR1	-4.00	CXCL5	-2.49
THBS1	-3.99	THBS1	-2.49
TEK	-3.95	TEK	-2.47
ANGPT1	-3.22	ANGPT1	-1.99
ITGAV	-3.17	SERPINF1	-1.99

D

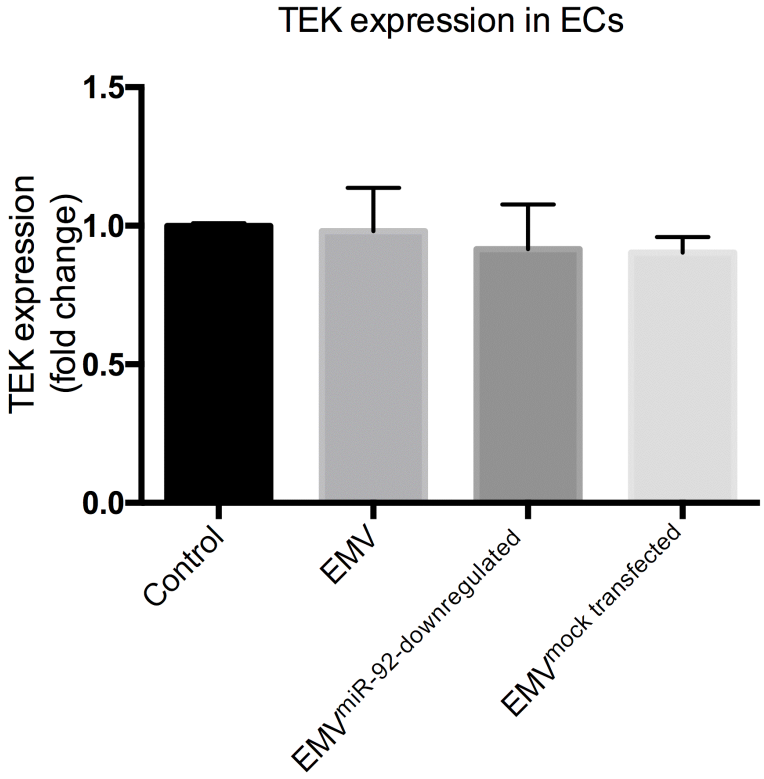

E

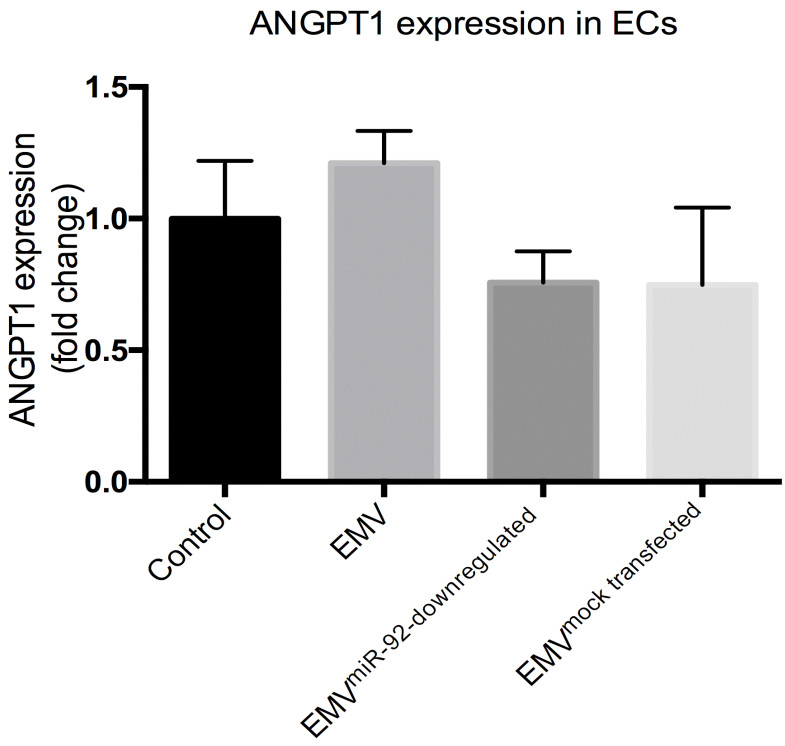
ANGPT1 expression in ECs
ANGPT1 expression (fold change)
1.5
1.0
0.5
0.0
Control
EMV
EMVmiR-92-downregulated
EMVmock transfected

F

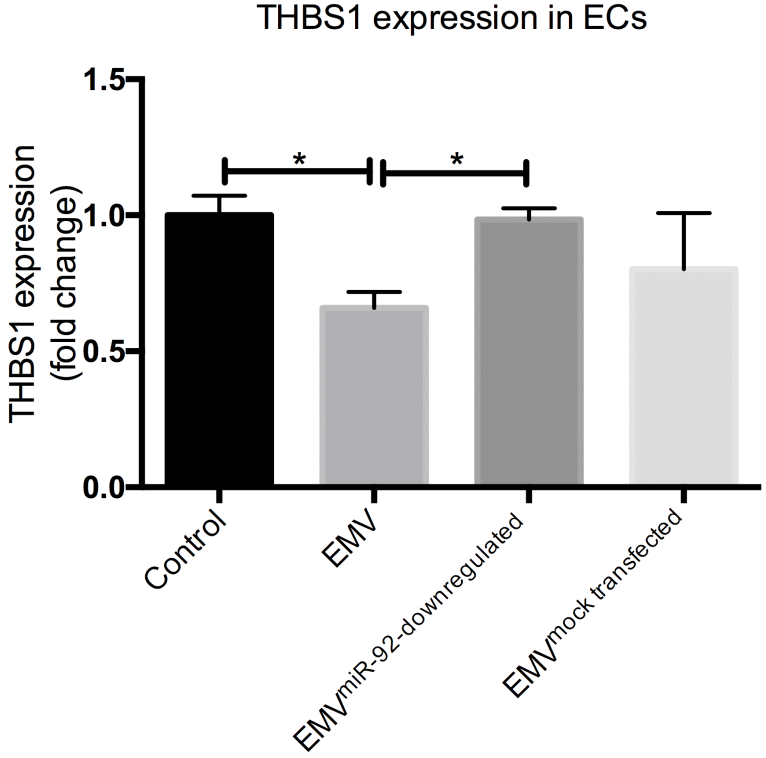
THBS1 expression in ECs
THBS1 expression (fold change)
1.5
1.0
0.5
0.0
*
*
Control
EMV
EMVmiR-92-downregulated
EMVmock transfected

G

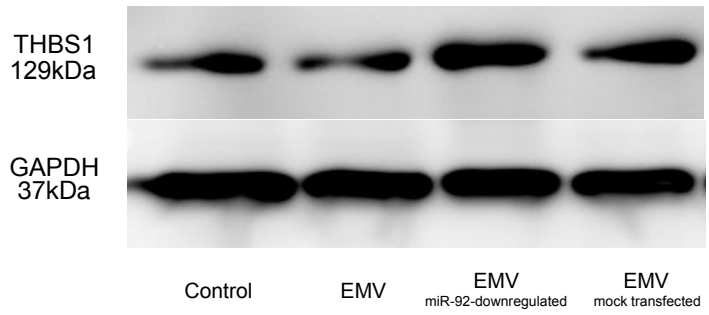

Fig. 10: EMV-incorporated miR-92 regulates angiogenesis in recipient ECs in a THBS1-dependent mechanism

ECs in basal media were co-incubated with EMV, EMV$^{miR\text{-}92\text{-}downregulated}$ or vehicle for 24 hours. (A) Scatter Plot showing differentially regulated genes after EMV and control treatment. The five strongest downregulated genes after EMV treatment are highlighted (n=3). (B) Scatter Plot showing differentially regulated genes between after EMV and EMV$^{miR\text{-}92\text{-}downregulated}$ treatment by PCR array. The five strongest downregulated genes after EMV treatment are highlighted (n=3). (C) Summary of the top 5 downregulated genes after EMV treatment compared to control and EMV$^{miR\text{-}92\text{-}downregulated}$. RPLP0 was used as endogenous control in PCR array. The grey background highlights the three genes which were downregulated by EMV in both analysis (compared to control and compared to EMV$^{miR\text{-}92\text{-}downregulated}$). (D) TEK expression of ECs that were treated with EMV, EMV$^{miR\text{-}92\text{-}downregulated}$, EMV$^{mock\text{-}transfected}$ or vehicle was determined by real-time PCR. (E) ANGPT1 expression of ECs that were treated with EMV, EMV$^{miR\text{-}92\text{-}downregulated}$, EMV$^{mock\text{-}transfected}$ or vehicle was determined by real-time PCR (n=3, by 1-way ANOVA with Bonferroni's multiple comparisons test). GAPDH was used as an endogenous control in real-time PCR. (F) THBS1 expression in target ECs that were treated with EMV, EMV$^{miR\text{-}92\text{-}downregulated}$, EMV$^{mock\text{-}transfected}$ or vehicle was determined by real-time PCR (*P<0.05, n=3, by 1-way ANOVA with Bonferroni's multiple comparisons test). GAPDH was used as an endogenous control. (G) THBS1 expression in target ECs that were treated with vehicle, EMV, EMV$^{miR\text{-}92\text{-}downregulated}$ or EMV$^{mock\text{-}transfected}$ was analyzed by western blot. EMV indicates endothelial cell-derived microvesicle; EC, endothelial cell; miR, microRNA; THBS1, thrombospondin 1; RPLP0,

ribosomal protein lateral stalk subunit P0. TEK, TEK Receptor Tyrosine Kinase and ANGPT1, angiopoietin 1.

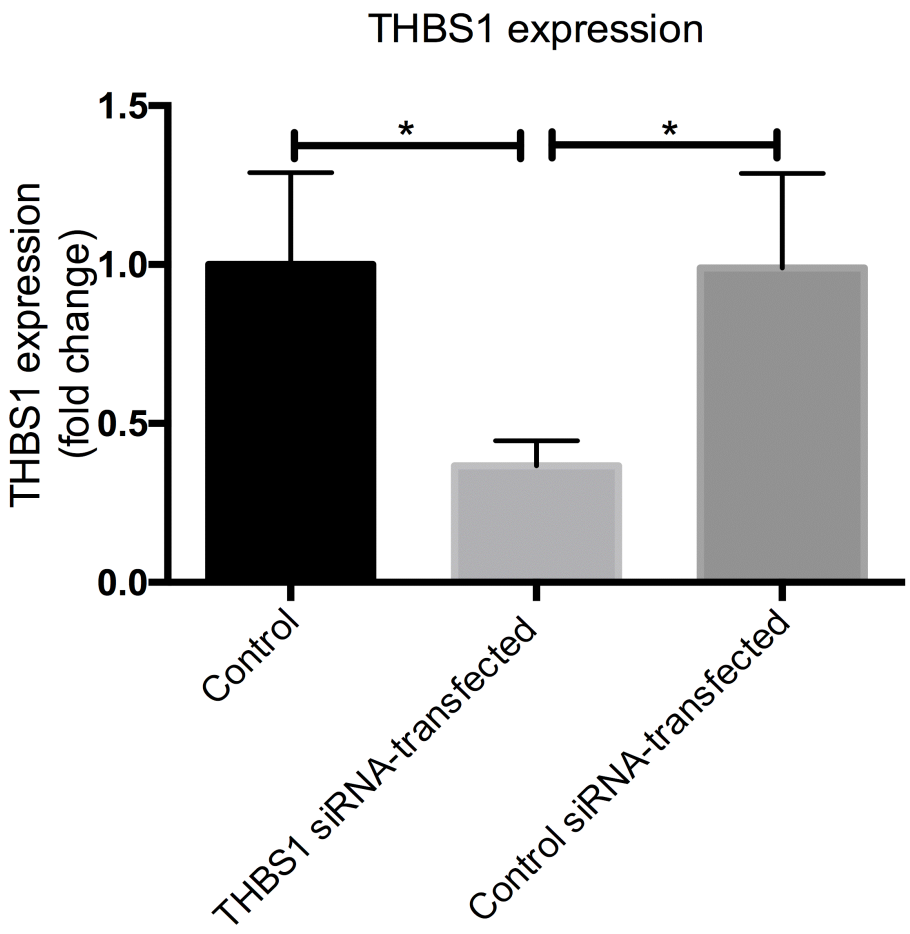

Fig. 11: THBS1 expression in ECs

ECs were transfected with THBS1 siRNA or scrambled control siRNA. Non-transfected ECs served as control. THBS1 expression was analyzed in ECs (*P<0.05, n=4, by 1-way ANOVA with Bonferroni's multiple comparisons test). GAPDH was used as an endogenous control. (*P<0.05, n=4, by 1-way ANOVA with Bonferroni's multiple comparisons test). EC indicates endothelial cell; THBS1, thrombospondin 1.

A

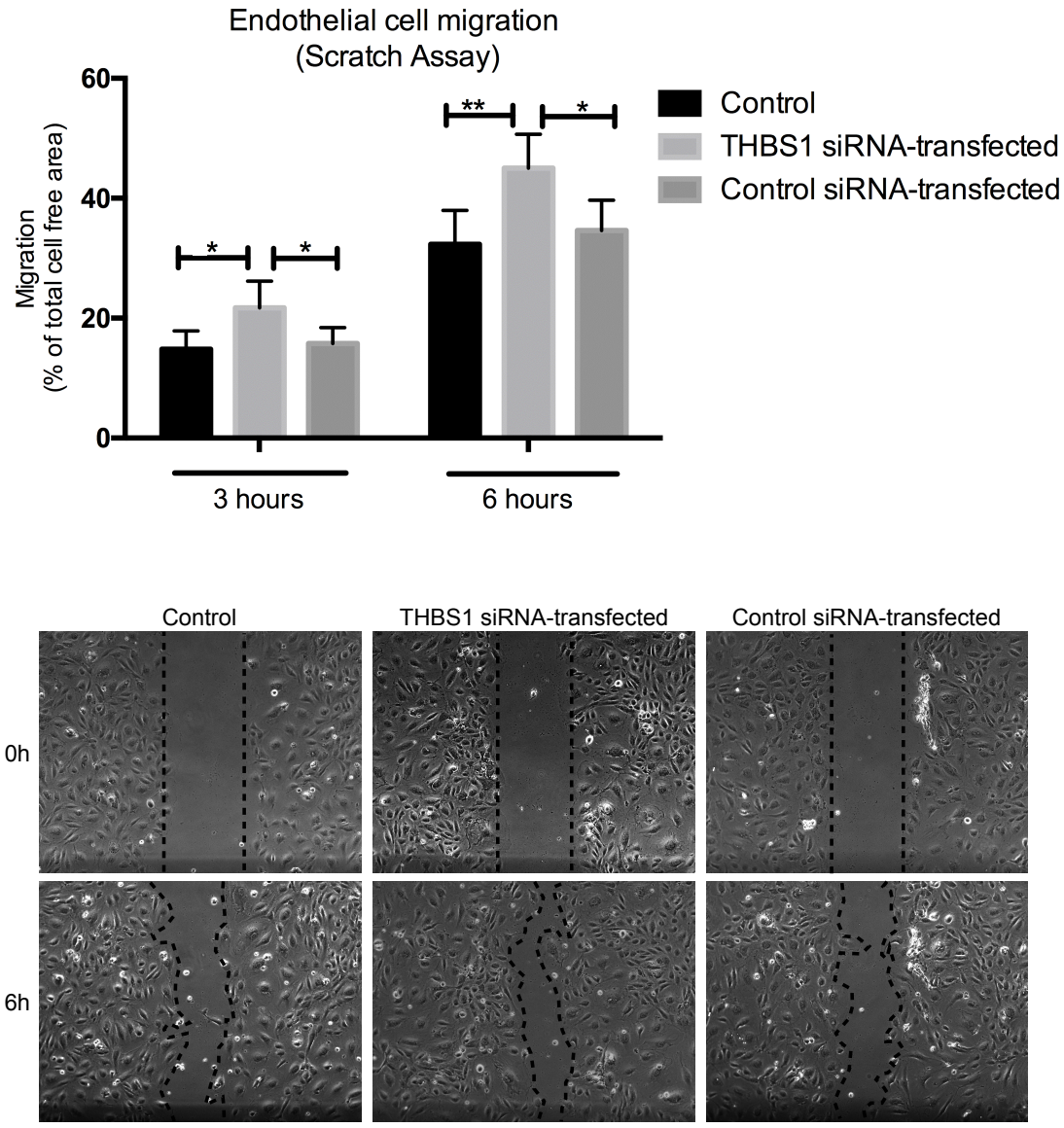
Endothelial cell migration
(Scratch Assay)
Migration
(% of total cell free area)
60
40
20
0
*
*
**
*
3 hours
6 hours
Control
THBS1 siRNA-transfected
Control siRNA-transfected
Control
THBS1 siRNA-transfected
Control siRNA-transfected
0h
6h

B

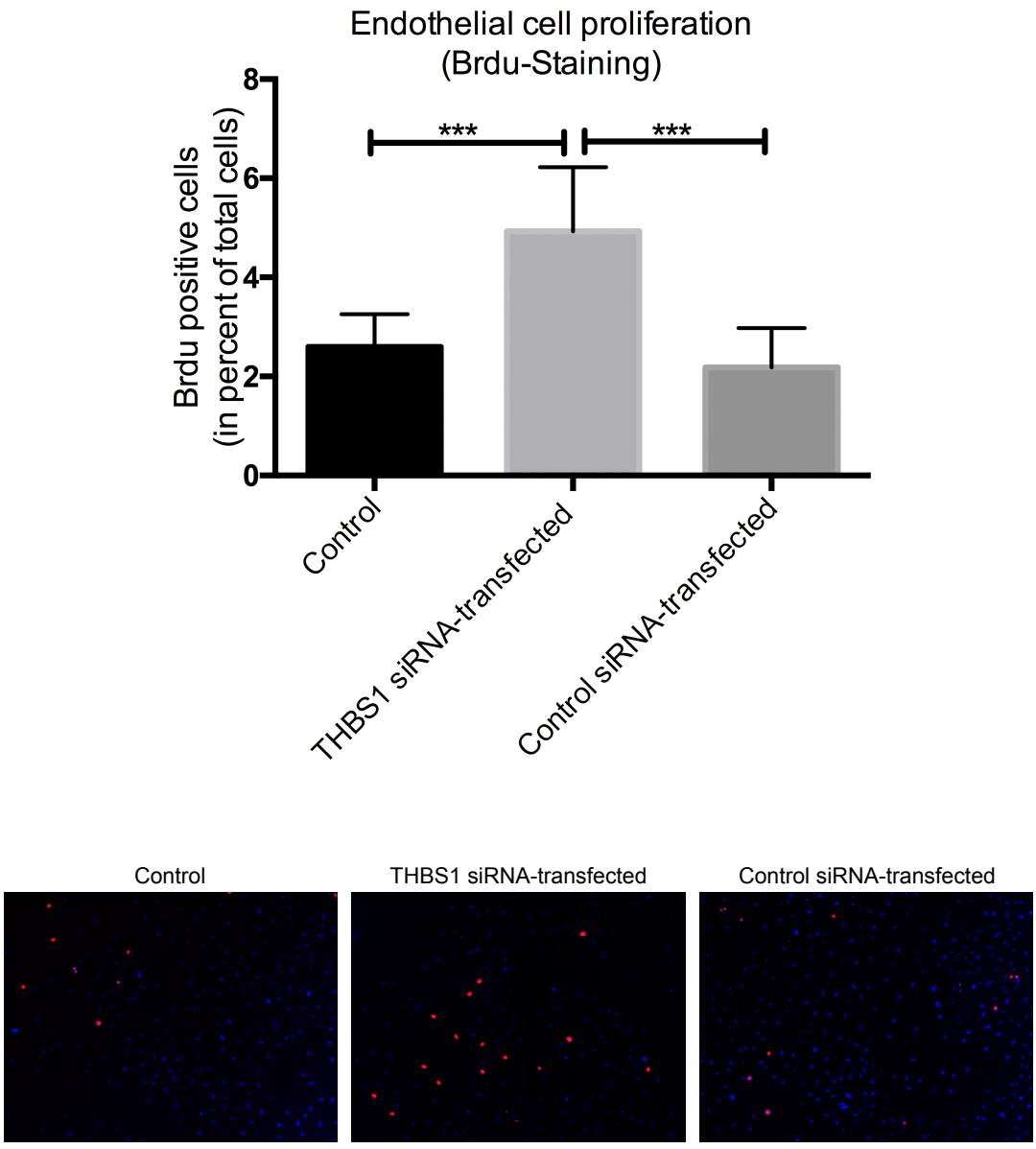

Fig. 12: THBS1 negatively regulates migration and proliferation in ECs

ECs were transfected with THBS1 siRNA or scrambled control siRNA. Non-transfected ECs served as control. (A) Scratch migration assay was performed and representative images of cells migrating into the scratched region were shown. Quantitative analysis of migration was measured as a percentage of total

cell-free area (*P<0.05, **P<0.01, n=6, by 1-way ANOVA with Bonferroni's multiple comparisons test). (B) BrdU incorporation was determined by immunofluorescence (red). Nuclei were stained with DAPI (blue). The percentage of BrdU-positive cells was compared (***P<0.001, n=10, by 1-way ANOVA with Bonferroni's multiple comparisons test). Magnification ×100. THBS1 indicates thrombospondin 1; EC, endothelial cell; BrdU, bromodeoxyuridine and DAPI, 4′,6-diamidino-2-phenylindole.

4. Discussion

miRs are currently explored as biomarkers in a wide range of cardiovascular conditions including atherosclerotic diseases. Circulating miRs are detectable and remarkably stable in body fluids such as blood and urine. Circulating MV represent major transport vehicles for miRs by separating them from circulating RNase(Boon and Vickers, 2013). Increasing evidence suggests that CAD patients show elevated levels of circulating MV, which might be actively involved in the progression of vascular dysfunction in atherosclerotic conditions(Jansen, et al., 2014). However, so far, the biological content of circulating MV in patients with or without CAD is vastly unknown.

MV-bound miRs, compared to freely circulating miRs, were shown to predict cardiovascular events in patients with stable CAD(Jansen, et al., 2014). Therefore, we focused on analyzing the expression of MV-incorporated miRs in this study. Analysis of circulating MV-miRs showed significantly increased levels of miR-92 in patients with stable CAD and ACS in comparison to patients without CAD. These findings emphasize a potential role for miR-transporting MV in the regulation of vascular health, which is altered under atherosclerotic conditions. Next, we further explored cellular origins of MV-bound miR-92 in CAD patients. It has been shown that miR-92 is highly expressed in various cell types, such as ECs, platelets and monocyte-lineage cells(Zhang, et al., 2014, Zhang, et al., 2015, Sisk, et al., 2012). The high expression of miR-92 in sorted patient-derived CD31+/CD42b- MV on one hand and in EC-derived EMV in vitro suggests that circulating MV-miR-92 is mainly of endothelial cell origin, which is in line with an increasing body of evidence(Zhang, et al., 2017, Chen, et al., 2014).

In analogy to our clinical findings, in vitro experiments demonstrated that miR-92 was dose-dependently up-regulated after oxLDL stimulation as pro-atherogenic stimulus in ECs and EC-derived EMV. Taken together, these findings emphasize that miR-92 is predominately upregulated in ECs and EMV in atherosclerotic conditions.

Previous studies have shown that miR-92 expression is controlled by a large variety of transcription factors(Concepcion, et al., 2012). In this context, miR-92 expression was upregulated by STAT3 in ECs and lung cancer cells(Loyer, et al., 2013, Lin, et al., 2013). However, whether STAT3 could be involved in the specific regulation of miR-92 in MV is

unknown. Our studies unveil a critical role for STAT3 in regulating miR-92 expression in MV in a dose-dependent way.

Evidence suggested that loss-of-function of miR-92 resulted in smaller embryos and immediate postnatal death of all animals. This was likely due to severely ventricular septal defects in the hearts of mice lacking miR-92(Mendell, 2008). Furthermore, miR-92 has been shown to be a crucial regulator of angiogenesis and vascular integrity. Daniel et al. showed that inhibition of miR-92 enhances re-endothelialization and prevents neointimal lesion formation after endovascular injury(Daniel, et al., 2014). In line with these findings, inhibition of miR-92 increased endothelial proliferation and migration in vitro and reduced neointimal formation after balloon injury or arterial stenting in vivo(Iaconetti, et al., 2012). Consistently, Hinkel et al. showed that an efficient inhibition of miR-92 exhibits pleiotropic beneficial effects, which may contribute to the improved recovery of heart function after ischemia/reperfusion injury in a preclinical pig model(Hinkel, et al., 2013). Taken together, these results demonstrate that miR-92 plays an important role in developmental and pathological angiogenesis. Whereas inhibition of miR-92 seems to mediate vascular regeneration and reduce vascular remodeling, the functional role of miR-92 in EMV is unclear. To explore whether EMV-incorporated miR-92 might play a functional role in the regulation of vascular performance, we first explored whether EMV-bound miR-92 was taken up by target ECs. By using Cy3-labeled miR-92 and PKH67-labeled EMV, we found that miR-92 was transferred via EMV into recipient ECs. Next, loss-of-function experiments showed that EMV promoted EC migration, proliferation and tube formation in a miR-92-dependent manner in vitro, which was abrogated by downregulation of miR-92 in EMV. Consistent with our results, Umezu et al have shown that exogenous miR-92 application via exosomes enhanced EC migration and tube formation(Umezu, et al., 2013). Conversely, Bonauer et al demonstrated that overexpression of miR-92 in ECs repressed angiogenesis both in vitro and vivo(Bonauer, et al., 2009). Based on our findings and the above evidence, intracellular levels of miR-92 in ECs can be in elevated in two ways: 1) direct upregulation using transfection of precursor miR-92; 2) delivery of exogenous miR-92 via biological transporting cargoes, e.g. exosomes or MV. Apparently, though the two ways both result in augmented cellular levels of miR-92, the subsequent cellular function and phenotype

can differ. In summary, the role of miR-92 in the regulation of angiogenesis is still controversial and may vary depending on the experimental model and methods of regulating miR-92.

miR-92 regulates angiogenesis and has multiple mRNA targets. Bonauer et al demonstrated that miR-92 could directly target integrin α5 (ITGA5) (Bonauer, et al., 2009). Likewise, Zhang et al demonstrated that phosphatase and tensin homolog (PTEN) is a direct target of miR-92, the PTEN plays a central role in regulating angiogenesis(Zhang, et al., 2014). Our PCR-based gene expression array results suggested that THBS1, TEK, ANGPT1 were downregulated by EMV-bound miR-92 in target ECs. However, single real-time PCR experiments revealed that only THBS1 was inhibited by EMV-miR-92. THBS1 has been one the first endogenous inhibitors of angiogenesis which has been identified(Tandle, et al., 2004). THBS1 inhibits angiogenesis directly by interacting with specific receptors and stimulating Fas/Fas ligand-mediated apoptosis of ECs, or indirectly by modulating the activity of several angiogenic factors(Italiano, et al., 2012). Interestingly, tumor angiogenesis is also associated with a significantly upregulated cellular expressions of miR-92, leading to downregulated THBS1, and the therapeutic efficacy of a THBS1 inhibitor has been evaluated in a phase 2 trial(Italiano, et al., 2012, Gordon, et al., 2008, Dews, et al., 2006). Finally, our functional in vitro experiments confirmed that THBS1 negatively regulates EC migration and proliferation, cellular processes mediating angiogenesis.

In summary, we show that clinical and experimental atherosclerotic conditions promote the packaging of miR-92 into EMV. EMV contain and transfer functional miR-92 into recipient ECs, inhibit THBS1 expression, and promote EC migration, proliferation and tube formation in a miR-92-dependent manner (Figure 13). These results indicate that EMV can act as biological vectors delivering functional miR-92 into recipient ECs. Based on our findings, one can speculate that pro-atherogenic stimuli promote the release of miR-92-containing EMV as a messenger carrying a potentially regenerative signal that can be taken up by EC further downstream in the blood to promote angiogenesis in conditions of vascular damage. These results add new aspects to the role and function of miR-92 in EMV as a potential regenerative messenger in intercellular communication. However, some important questions remain and will be addressed in future studies. First,

the analysis of circulating miRs bound to other cargos than MV (e.g. HDL or Ago proteins) would be of interest for future studies. Second, only a selected number of miRs, based on own array results and previously published data, were analyzed. Finally, although we see a specific effect of miR-92 in EMV, we cannot rule out the influence of other miRs or bioactive molecules present in EMV in our findings.

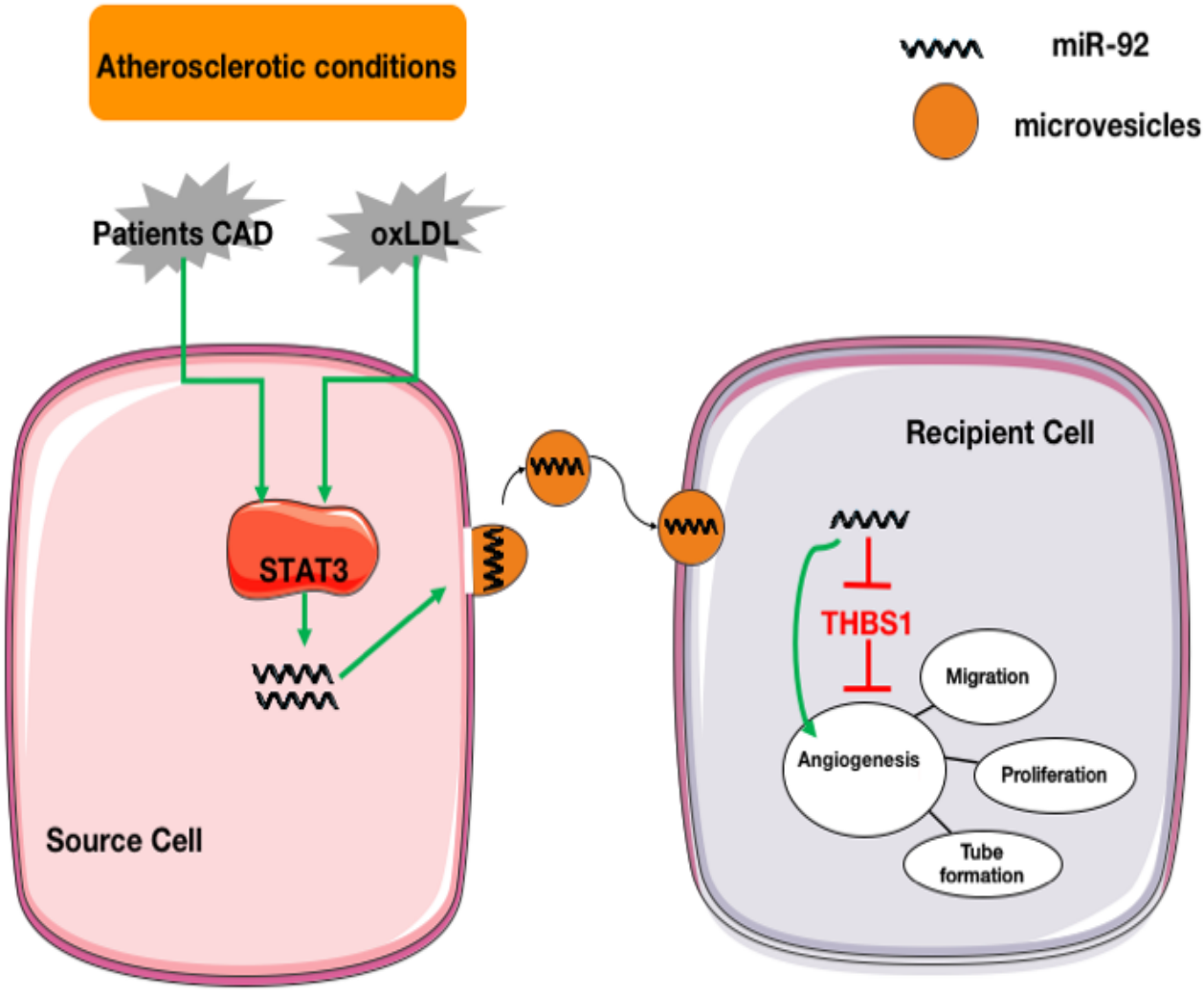

Fig. 13: Proposed mechanism

In atherosclerotic conditions, miR-92 expression both in ECs and EMV is upregulated in a STAT3-dependent way. EMV released from parent ECs contain and transfer miR-92 into adjacent ECs.

MiR-92-mediated inhibition of THBS1 promotes adjacent ECs migration, proliferation and angiogenesis. ECs indicates endothelial cells; EMV indicates endothelial cell-derived microvesicle; THBS1 indicates thrombospondin 1.

5. Conclusion

In this study, we provide evidence that clinical and experimental atherosclerotic conditions promote the packaging of functional miR-92 into MV. EMV-mediated transfer of functional miR-92 regulates angiogenesis in recipient ECs in a THBS1-dependent mechanism.

6. Summary

Whether MV-miR expression is regulated in coronary artery disease (CAD) or not is unknown. We aimed to explore the expression of circulating MV-miRs in patients with CAD.

A Taqman miR array revealed that certain MV-miRs are significantly regulated in patients with stable CAD compared to ACS patients. 180 patients with angiographically excluded CAD (n=41), stable CAD (n=77), and acute coronary syndrome (ACS, n=62) were prospectively studied. Nine miRs involved in the regulation of vascular performance were quantified in circulating MVs. Among these, miR-92 was significantly increased in patients with CAD compared to non-CAD patients. In vitro, oxLDL stimulation increased miR-92 expression in parent ECs and endothelial microvesicle (EMV). Labeling of miR-92 and EMVs demonstrated miR-92 was transported into recipient ECs. Knockdown of miR-92 in EMVs abrogated EMV-mediated effects on EC migration and proliferation and blocked vascular network formation in a matrigel plug. PCR-based gene profiling showed that the expression of THBS1 protein, a target of miR-92 and an inhibitor of angiogenesis, was significantly reduced in ECs by EMV. Knockdown of miR-92 in EMV abrogated EMV-mediated inhibition of the THBS1 gene and protein expression.

In summary, we provide evidence that microvesicles-incorporated miR-92 is upregulated in patients with coronary artery disease. In vitro, oxidized LDL promotes the packaging of functional microRNA-92 from endothelial cells into microvesicles promoting angiogenic responses in recipient cells in a THBS1-dependent manner.

7. List of Figures

8. List of Tables

9. References

Amabile N, Guérin AP, Leroyer A, Mallat Z, Nguyen C, Boddaert J, London GM, Tedgui A, Boulanger CM. Circulating endothelial microparticles are associated with vascular dysfunction in patients with end-stage renal failure. Journal of the American Society of Nephrology. 2005. 16: 3381-3388

Arroyo JD, Chevillet JR, Kroh EM, Ruf IK, Pritchard CC, Gibson DF, Mitchell PS, Bennett CF, Pogosova-Agadjanyan EL, Stirewalt DL. Argonaute2 complexes carry a population of circulating microRNAs independent of vesicles in human plasma. Proceedings of the National Academy of Sciences. 2011. 108: 5003-5008

Bernal-Mizrachi L, Jy W, Fierro C, Macdonough R, Velazques HA, Purow J, Jimenez JJ, Horstman LL, Ferreira A, De Marchena E. Endothelial microparticles correlate with high-risk angiographic lesions in acute coronary syndromes. International journal of cardiology. 2004. 97: 439-446

Bonauer A, Carmona G, Iwasaki M, Mione M, Koyanagi M, Fischer A, Burchfield J, Fox H, Doebele C, Ohtani K. MicroRNA-92a controls angiogenesis and functional recovery of ischemic tissues in mice. Science. 2009. 324: 1710-1713

Boon RA, Vickers KC. Intercellular transport of microRNAs. Arteriosclerosis, thrombosis, and vascular biology. 2013. 33: 186-192

Boulanger CM, Amabile N, Tedgui A. Circulating microparticles: a potential prognostic marker for atherosclerotic vascular disease. Hypertension. 2006. 48: 180-186

Boulanger CM, Loyer X, Rautou P-E, Amabile N. Extracellular vesicles in coronary artery disease. Nature reviews cardiology. 2017. 14: 259

Boulanger CM, Rautou P-E, Vion A-C, Amabile N, Chironi G, Simon A, Tedgui A.

Microparticles, vascular function and atherothrombosis. Vascular Pharmacology. 2012. 56: 318

Brill A, Dashevsky O, Rivo J, Gozal Y, Varon D. Platelet-derived microparticles induce angiogenesis and stimulate post-ischemic revascularization. Cardiovascular research. 2005. 67: 30-38

Brock M, Trenkmann M, Gay RE, Gay S, Speich R, Huber LC. MicroRNA-18a enhances the interleukin-6-mediated production of the acute-phase proteins fibrinogen and haptoglobin in human hepatocytes. Journal of Biological Chemistry. 2011. 286: 40142-40150

Brogan P, Shah V, Brachet C, Harnden A, Mant D, Klein N, Dillon M. Endothelial and platelet microparticles in vasculitis of the young. Arthritis & Rheumatology. 2004. 50: 927-936

Camussi G, Deregibus MC, Bruno S, Cantaluppi V, Biancone L. Exosomes/microvesicles as a mechanism of cell-to-cell communication. Kidney international. 2010. 78: 838-848

Chen M, Ma G, Yue Y, Wei Y, Li Q, Tong Z, Zhang L, Miao G, Zhang J. Downregulation of the miR-30 family microRNAs contributes to endoplasmic reticulum stress in cardiac muscle and vascular smooth muscle cells. International journal of cardiology. 2014. 173: 65-73

Chen M, Masaki T, Sawamura T. LOX-1, the receptor for oxidized low-density lipoprotein identified from endothelial cells: implications in endothelial dysfunction and atherosclerosis. Pharmacology & therapeutics. 2002. 95: 89-100

Chen Z, Wen L, Martin M, Hsu C-Y, Fang L, Lin F-M, Lin T-Y, Geary MJ, Geary G, Zhao Y. Oxidative stress activates endothelial innate immunity via sterol regulatory element binding protein 2 (srebp2) transactivation of mirna-92a. Circulation. 2014.

CIRCULATIONAHA. 114.013675

Chironi G, Simon A, Hugel B, Del Pino M, Gariepy J, Freyssinet J-M, Tedgui A. Circulating leukocyte-derived microparticles predict subclinical atherosclerosis burden in asymptomatic subjects. Arteriosclerosis, thrombosis, and vascular biology. 2006. 26: 2775-2780

Concepcion CP, Bonetti C, Ventura A. The miR-17-92 family of microRNA clusters in development and disease. Cancer journal (Sudbury, Mass). 2012. 18: 262

Corsten MF, Dennert R, Jochems S, Kuznetsova T, Devaux Y, Hofstra L, Wagner DR, Staessen J, Heymans S, Schroen B. Circulating MicroRNA-208b and MicroRNA-499 reflect myocardial damage in cardiovascular disease. Circulation: Genomic and Precision Medicine. 2010. CIRCGENETICS. 110.957415

Daniel J-M, Penzkofer D, Teske R, Dutzmann J, Koch A, Bielenberg W, Bonauer A, Boon RA, Fischer A, Bauersachs J. Inhibition of miR-92a improves re-endothelialization and prevents neointima formation following vascular injury. Cardiovascular research. 2014. 103: 564-572

Del Conde I, Shrimpton CN, Thiagarajan P, López JA. Tissue-factor–bearing microvesicles arise from lipid rafts and fuse with activated platelets to initiate coagulation. Blood. 2005. 106: 1604-1611

Dews M, Homayouni A, Yu D, Murphy D, Sevignani C, Wentzel E, Furth EE, Lee WM, Enders GH, Mendell JT. Augmentation of tumor angiogenesis by a Myc-activated microRNA cluster. Nature genetics. 2006. 38: 1060-1065

Dignat-George F, Camoin-Jau L, Sabatier F, Arnoux D, Anfosso F, Bardin N, Veit V, Combes V, Gentile S, Moal V. Endothelial microparticles: a potential contribution to the thrombotic complications of the antiphospholipid syndrome. Thrombosis and

haemostasis. 2004. 92: 667-673

Esposito K, Ciotola M, Schisano B, Gualdiero R, Sardelli L, Misso L, Giannetti G, Giugliano D. Endothelial microparticles correlate with endothelial dysfunction in obese women. The Journal of Clinical Endocrinology & Metabolism. 2006. 91: 3676-3679

Fichtlscherer S, De Rosa S, Fox H, Schwietz T, Fischer A, Liebetrau C, Weber M, Hamm CW, Röxe T, Müller-Ardogan M. Circulating microRNAs in patients with coronary artery diseasenovelty and significance. Circulation research. 2010. 107: 677-684

García-Conesa MT, Tribolo S, Guyot S, Tomás-Barberán FA, Kroon PA. Oligomeric procyanidins inhibit cell migration and modulate the expression of migration and proliferation associated genes in human umbilical vascular endothelial cells. Molecular nutrition & food research. 2009. 53: 266-276

Gomes Da Silva AM, Silbiger VN. miRNAs as biomarkers of atrial fibrillation. Biomarkers. 2014. 19: 631-636

González-Quintero VcH, Jiménez JnJ, Jy W, Mauro LaM, Hortman L, O'sullivan MJ, Ahn Y. Elevated plasma endothelial microparticles in preeclampsia. American Journal of Obstetrics & Gynecology. 2003. 189: 589-593

Gordon MS, Mendelson D, Carr R, Knight RA, Humerickhouse RA, Iannone M, Stopeck AT. A phase 1 trial of 2 dose schedules of ABT-510, an antiangiogenic, thrombospondin-1-mimetic peptide, in patients with advanced cancer. Cancer. 2008. 113: 3420-3429

György B, Módos K, Pállinger É, Pálóczi K, Pásztói M, Misják P, Deli MA, Sipos Á, Szalai A, Voszka I. Detection and isolation of cell-derived microparticles are compromised by protein complexes resulting from shared biophysical parameters. Blood. 2011. 117: e39-e48

Heiss C, Amabile N, Lee AC, Real WM, Schick SF, Lao D, Wong ML, Jahn S, Angeli FS, Minasi P. Brief secondhand smoke exposure depresses endothelial progenitor cells activity and endothelial function: sustained vascular injury and blunted nitric oxide production. Journal of the American College of Cardiology. 2008. 51: 1760-1771

Hergenreider E, Heydt S, Tréguer K, Boettger T, Horrevoets AJ, Zeiher AM, Scheffer MP, Frangakis AS, Yin X, Mayr M. Atheroprotective communication between endothelial cells and smooth muscle cells through miRNAs. Nature cell biology. 2012. 14: 249

Hinkel R, Penzkofer D, Zühlke S, Fischer A, Husada W, Xu Q-F, Baloch E, Van Rooij E, Zeiher AM, Kupatt C. Inhibition of microRNA-92a protects against ischemia-reperfusion injury in a large animal model. Circulation. 2013. CIRCULATIONAHA. 113.001904

Iaconetti C, Polimeni A, Sorrentino S, Sabatino J, Pironti G, Esposito G, Curcio A, Indolfi C. Inhibition of miR-92a increases endothelial proliferation and migration in vitro as well as reduces neointimal proliferation in vivo after vascular injury. Basic research in cardiology. 2012. 107: 296

Italiano A, Thomas R, Breen M, Zhang L, Crago AM, Singer S, Khanin R, Maki RG, Mihailovic A, Hafner M. The miR-17-92 cluster and its target THBS1 are differentially expressed in angiosarcomas dependent on MYC amplification. Genes, Chromosomes and Cancer. 2012. 51: 569-578

Jansen F, Wang H, Przybilla D, Franklin BS, Dolf A, Pfeifer P, Schmitz T, Flender A, Endl E, Nickenig G. Vascular endothelial microparticles-incorporated microRNAs are altered in patients with diabetes mellitus. Cardiovascular diabetology. 2016. 15: 49

Jansen F, Yang X, Baumann K, Przybilla D, Schmitz T, Flender A, Paul K, Alhusseiny A, Nickenig G, Werner N. Endothelial microparticles reduce ICAM-1 expression in a microRNA-222-dependent mechanism. Journal of cellular and molecular medicine. 2015. 19: 2202-2214

Jansen F, Yang X, Hoelscher M, Cattelan A, Schmitz T, Proebsting S, Wenzel D, Vosen S, Franklin BS, Fleischmann BK. Endothelial microparticle-mediated transfer of MicroRNA-126 promotes vascular endothelial cell repair via SPRED1 and is abrogated in glucose-damaged endothelial microparticles. Circulation. 2013. CIRCULATIONAHA. 113.001720

Jansen F, Yang X, Hoyer FF, Paul K, Heiermann N, Becher MU, Hussein NA, Kebschull M, Bedorf J, Franklin BS. Endothelial microparticle uptake in target cells is annexin I/phosphatidylserine receptor dependent and prevents apoptosis. Arteriosclerosis, thrombosis, and vascular biology. 2012. 32: 1925-1935

Jansen F, Yang X, Proebsting S, Hoelscher M, Przybilla D, Baumann K, Schmitz T, Dolf A, Endl E, Franklin BS. MicroRNA expression in circulating microvesicles predicts cardiovascular events in patients with coronary artery disease. Journal of the American Heart Association. 2014. 3: e001249

Jansen F, Zietzer A, Stumpf T, Flender A, Schmitz T, Nickenig G, Werner N. Endothelial microparticle-promoted inhibition of vascular remodeling is abrogated under hyperglycaemic conditions. Journal of molecular and cellular cardiology. 2017. 112: 91-94

Jayachandran M, Litwiller RD, Owen WG, Heit JA, Behrenbeck T, Mulvagh SL, Araoz PA, Budoff MJ, Harman SM, Miller VM. Characterization of blood borne microparticles as markers of premature coronary calcification in newly menopausal women. American Journal of Physiology-Heart and Circulatory Physiology. 2008. 295: H931-H938

Köberle V, Pleli T, Schmithals C, Alonso EA, Haupenthal J, Bönig H, Peveling-Oberhag J, Biondi RM, Zeuzem S, Kronenberger B. Differential stability of cell-free circulating microRNAs: implications for their utilization as biomarkers. PloS one. 2013. 8: e75184

Koga H, Sugiyama S, Kugiyama K, Watanabe K, Fukushima H, Tanaka T, Sakamoto T,

Yoshimura M, Jinnouchi H, Ogawa H. Elevated levels of VE-cadherin-positive endothelial microparticles in patients with type 2 diabetes mellitus and coronary artery disease. Journal of the American College of Cardiology. 2005. 45: 1622-1630

Lee RC, Ambros V. An extensive class of small RNAs in Caenorhabditis elegans. Science. 2001. 294: 862-864

Lee RC, Feinbaum RL, Ambros V. The C. elegans heterochronic gene lin-4 encodes small RNAs with antisense complementarity to lin-14. cell. 1993. 75: 843-854

Lerman A, Zeiher AM. Endothelial function: cardiac events. Circulation. 2005. 111: 363-368

Lin H, Chiang C, Hung W. STAT3 upregulates miR-92a to inhibit RECK expression and to promote invasiveness of lung cancer cells. British journal of cancer. 2013. 109: 731-738

Loyer X, Potteaux S, Vion A-C, Guérin CL, Boulkroun S, Rautou P-E, Ramkhelawon B, Esposito B, Dalloz M, Paul J-L. Inhibition of microRNA-92a prevents endothelial dysfunction and atherosclerosis in mice. Circulation research. 2013. CIRCRESAHA. 113.302213

Loyer X, Vion A-C, Tedgui A, Boulanger CM. Microvesicles as cell–cell messengers in cardiovascular diseases. Circulation research. 2014. 114: 345-353

Mallat Z, Benamer H, Hugel B, Benessiano J, Steg PG, Freyssinet J-M, Tedgui A. Elevated levels of shed membrane microparticles with procoagulant potential in the peripheral circulating blood of patients with acute coronary syndromes. Circulation. 2000. 101: 841-843

Mendell JT. miRiad roles for the miR-17-92 cluster in development and disease. Cell. 2008. 133: 217-222

Owens AP, Mackman N. Microparticles in hemostasis and thrombosis. Circulation research. 2011. 108: 1284-1297

Pirillo A, Norata GD, Catapano AL. LOX-1, OxLDL, and atherosclerosis. Mediators of inflammation. 2013. 2013

Rane S, He M, Sayed D, Vashistha H, Malhotra A, Sadoshima J, Vatner DE, Vatner SF, Abdellatif M. Downregulation of miR-199a derepresses hypoxia-inducible factor-1α and Sirtuin 1 and recapitulates hypoxia preconditioning in cardiac myocytes. Circulation research. 2009. 104: 879-886

Rautou P-E, Vion A-C, Amabile N, Chironi G, Simon A, Tedgui A, Boulanger CM. Microparticles, vascular function, and atherothrombosis. Circulation research. 2011. 109: 593-606

Ray DM, Spinelli SL, Pollock SJ, Murant TI, O'brien JJ, Blumberg N, Francis CW, Taubman MB, Phipps RP. Peroxisome proliferator-activated receptor γ and retinoid X receptor transcription factors are released from activated human platelets and shed in microparticles. Thrombosis and haemostasis. 2008. 99: 86-95

Schiro A, Wilkinson F, Weston R, Smyth J, Serracino-Inglott F, Alexander M. Endothelial microparticles as conveyors of information in atherosclerotic disease. Atherosclerosis. 2014. 234: 295-302

Shantsila E, Kamphuisen P, Lip G. Circulating microparticles in cardiovascular disease: implications for atherogenesis and atherothrombosis. Journal of Thrombosis and Haemostasis. 2010. 8: 2358-2368

Shen Y, Shen Z, Miao L, Xin X, Lin S, Zhu Y, Guo W, Zhu YZ. miRNA-30 family inhibition protects against cardiac ischemic injury by regulating cystathionine-γ-lyase expression.

Antioxidants & redox signaling. 2015. 22: 224-240

Siljander PR. Platelet-derived microparticles–an updated perspective. Thrombosis research. 2011. 127: S30-S33

Simak J, Gelderman M, Yu H, Wright V, Baird A. Circulating endothelial microparticles in acute ischemic stroke: a link to severity, lesion volume and outcome. Journal of thrombosis and haemostasis. 2006. 4: 1296-1302

Sisk JM, Clements JE, Witwer KW. miRNA profiles of monocyte-lineage cells are consistent with complicated roles in HIV-1 restriction. Viruses. 2012. 4: 1844-1864

Small EM, Frost RJ, Olson EN. MicroRNAs add a new dimension to cardiovascular disease. Circulation. 2010. 121: 1022-1032

Tandle A, Blazer DG, Libutti SK. Antiangiogenic gene therapy of cancer: recent developments. Journal of translational medicine. 2004. 2: 22

Thum T, Gross C, Fiedler J, Fischer T, Kissler S, Bussen M, Galuppo P, Just S, Rottbauer W, Frantz S. MicroRNA-21 contributes to myocardial disease by stimulating MAP kinase signalling in fibroblasts. Nature. 2008. 456: 980-984

Turchinovich A, Weiz L, Langheinz A, Burwinkel B. Characterization of extracellular circulating microRNA. Nucleic acids research. 2011. 39: 7223-7233

Umezu T, Ohyashiki K, Kuroda M, Ohyashiki J. Leukemia cell to endothelial cell communication via exosomal miRNAs. Oncogene. 2013. 32: 2747-2755

Voellenkle C, Van Rooij J, Cappuzzello C, Greco S, Arcelli D, Di Vito L, Melillo G, Rigolini R, Costa E, Crea F. MicroRNA signatures in peripheral blood mononuclear cells of chronic heart failure patients. Physiological genomics. 2010. 42: 420-426

Wang H, Wang Z-H, Kong J, Yang M-Y, Jiang G-H, Wang X-P, Zhong M, Zhang Y, Deng J-T, Zhang W. Oxidized Low-Density Lipoprotein–Dependent Platelet-Derived Microvesicles Trigger Procoagulant Effects and Amplify Oxidative Stress. Molecular medicine. 2012. 18: 159

Werner N, Wassmann S, Ahlers P, Kosiol S, Nickenig G. Circulating CD31+/annexin V+ apoptotic microparticles correlate with coronary endothelial function in patients with coronary artery disease. Arteriosclerosis, thrombosis, and vascular biology. 2006. 26: 112-116

Yu M-L, Wang J-F, Wang G-K, You X-H, Zhao X-X, Jing Q, Qin Y-W. Vascular smooth muscle cell proliferation is influenced by let-7d microRNA and its interaction with KRAS. Circulation Journal. 2011. 75: 703-709

Zernecke A, Bidzhekov K, Noels H, Shagdarsuren E, Gan L, Denecke B, Hristov M, Köppel T, Jahantigh MN, Lutgens E. Delivery of microRNA-126 by apoptotic bodies induces CXCL12-dependent vascular protection. Sci Signal. 2009. 2: ra81-ra81

Zhang L, Zhou M, Qin G, Weintraub NL, Tang Y. MiR-92a regulates viability and angiogenesis of endothelial cells under oxidative stress. Biochemical and biophysical research communications. 2014. 446: 952-958

Zhang Y, Cheng J, Chen F, Wu C, Zhang J, Ren X, Pan Y, Nie B, Li Q, Li Y. Circulating endothelial microparticles and miR-92a in acute myocardial infarction. Bioscience Reports. 2017. 37: BSR20170047

Zhang Y, Guan Q, Jin X. Platelet-derived miR-92a downregulates cysteine protease inhibitor cystatin C in type II diabetic lower limb ischemia. Experimental and therapeutic medicine. 2015. 9: 2257-2262

Zhang Y, Liu D, Chen X, Li J, Li L, Bian Z, Sun F, Lu J, Yin Y, Cai X. Secreted monocytic miR-150 enhances targeted endothelial cell migration. Molecular cell. 2010. 39: 133-144

10. Acknowledgments

I would like to express my gratitude to all those who helped me during the writing of this thesis.

First and foremost, I gratefully acknowledge the help of my supervisor, Professor Nikos Werner, who has offered me valuable suggestion in the process of research.

Second, I devote my high appreciations to Dr. Felix Jansen. He is a great mentor and supervisor. Without his patient instruction, insightful criticism and expert guidance, the completion of this thesis would not have been possible.

Most importantly, I want to express my thanks to Theresa Schmitz and Anna Flender, without their patient assistance and friendly encouragement, it would not be possible for me to complete this thesis in such a short period of time.

I also want to thank Chinese scholarship of China committee for their economic support.

Last but not least, I would like to express my special thanks to my parents, whose care and support motivate me to move on and make me want to be a better person.